diseases in Japan. *Intern Med* 1992; **31:** 304–309.
8. Koseki Y, Watanabe J, Shinozaki T, Sakuma M, Komaru T, Fukuchi M, et al. Characteristics and 1-year prognosis of medically treated patients with chronic heart failure in Japan. *Circ J* 2003; **67:** 431–436.
9. Tsuchihashi M, Tsutsui H, Kodama K, Kasagi F, Takeshita A. Clinical characteristics and prognosis of hospitalized patients with congestive heart failure: A study in Fukuoka, Japan. *Jpn Circ J* 2000; **64:** 953–959.
10. Tsuchihashi M, Tsutsui H, Kodama K, Kasagi F, Setoguchi S, Mohr M, et al. Medical and socioenvironmental predictors of hospital readmission in patients with congestive heart failure. *Am Heart J* 2001; **142:** E7.
11. Tsutsui H, Tsuchihashi M, Takeshita A. Mortality and readmission of hospitalized patients with congestive heart failure and preserved versus depressed systolic function. *Am J Cardiol* 2001; **88:** 530–533.
12. Ho KK, Anderson KM, Kannel WB, Grossman W, Levy D. Survival after the onset of congestive heart failure in Framingham Heart Study subjects. *Circulation* 1993; **88:** 107–115.
13. Kannel WB, Belanger AJ. Epidemiology of heart failure. *Am Heart J* 1991; **121:** 951–957.
14. Cowie MR, Wood DA, Coats AJ, Thompson SG, Poole-Wilson PA, Suresh V, et al. Incidence and aetiology of heart failure: A population-based study. *Eur Heart J* 1999; **20:** 421–428.
15. Krumholz HM, Parent EM, Tu N, Vaccarino V, Wang Y, Radford MJ, et al. Readmission after hospitalization for congestive heart failure among Medicare beneficiaries. *Arch Intern Med* 1997; **157:** 99–104.
16. Chin MH, Goldman L. Correlates of early hospital readmission or death in patients with congestive heart failure. *Am J Cardiol* 1997; **79:** 1640–1644.
17. Clarke KW, Gray D, Hampton JR. Evidence of inadequate investigation and treatment of patients with heart failure. *Br Heart J* 1994; **71:** 584–587.
18. Nielsen OW, Hilden J, Larsen CT, Hansen JF. Cross sectional study estimating prevalence of heart failure and left ventricular systolic dysfunction in community patients at risk. *Heart* 2001; **86:** 172–178.
19. Mair FS, Crowley TS, Bundred PE. Prevalence, aetiology and management of heart failure in general practice. *Br J Gen Pract* 1996; **46:** 77–79.
20. Morgan S, Smith H, Simpson I, Liddiard GS, Raphael H, Pickering RM, et al. Prevalence and clinical characteristics of left ventricular dysfunction among elderly patients in general practice setting: Cross sectional survey. *BMJ* 1999; **318:** 368–372.
21. The CONSENSUS Trial Study Group. Effects of enalapril on mortality in severe congestive heart failure: Results of the Cooperative North Scandinavian Enalapril Survival Study (CONSENSUS). *N Engl J Med* 1987; **316:** 1429–1435.
22. The SOLVD Investigators. Effect of enalapril on survival in patients with reduced left ventricular ejection fractions and congestive heart failure. *N Engl J Med* 1991; **325:** 293–302.

Appendix 1

JCARE-GENERAL Investigators
Principal Investigators: Akira Takeshita (Aso Iizuka Hospital); Hiroyuki Tsutsui (Hokkaido University).
Coinvestigators
Hakodate area: Hiroshi Okamoto (Hokkaido University); Akira Kitabatake (Showa Hospital; Past President of the Japanese Circulation Society and Past President of the Japanese Society of Heart Failure).
Shiogama area: Kunio Shirato (Saito Hospital); Tsuyoshi Shinozaki (National Hospital Organization Sendai Medical Center); Jun Watanabe (On-naduka Medical Office).
Mishima area: Mitsuaki Isobe (Tokyo Medical and Dental University); Yasuhiro Sato (National Hospital Organization Disaster Medical Center); Hiroshi Ito (Akita University).
Ishikawa Kahoku area: Noboru Takekoshi (Kanazawa Medical University); Takayoshi Asaji (Kanazawa Medical University).
Gifu Motosu area: Hisayoshi Fujiwara (Gifu University); Kazuhiko Nishigaki (Gifu University).
Ibaraki area: Masatsugu Hori (Osaka University; President of the Japanese Society of Heart Failure); Kazuhiro Yamamoto (Osaka University).
Kasai area: Mitsuhiro Yokoyama (Kobe University); Seinosuke Kawashima (Kobe University); Hiroshi Yamabe (Kasai City Hospital).
Kochi Hata area: Yoshinori Doi (Kochi University); Jun Takata (Kochi University).
Ube area: Masunori Matsuzaki (Yamaguchi University; President of the Japanese College of Cardiology); Masafumi Yano (Yamaguchi University).
Fukuoka Higashi area: Hiroyuki Tsutsui (Hokkaido University); Miyuki Tsuchihashi-Makaya (International Medical Center of Japan).
Kurume area: Tsutomu Imaizumi (Kurume University); Hisashi Kai (Kurume University).
Coordinators: Satoko Abe (Hokkaido University); Mayumi Koasa (Hokkaido University).

Cardiac-Specific Overexpression of Diacylglycerol Kinase ζ Prevents Gq Protein–Coupled Receptor Agonist–Induced Cardiac Hypertrophy in Transgenic Mice

Takanori Arimoto, MD; Yasuchika Takeishi, MD; Hiroki Takahashi, MD; Tetsuro Shishido, MD; Takeshi Niizeki, MD; Yo Koyama, MD; Ryoko Shiga, MD; Naoki Nozaki, MD; Osamu Nakajima, PhD; Kazuhide Nishimaru, PhD; Jun-ichi Abe, MD; Masao Endoh, MD; Richard A. Walsh, MD; Kaoru Goto, MD; Isao Kubota, MD

Background—Diacylglycerol is a lipid second messenger that accumulates in cardiomyocytes when stimulated by Gqα protein–coupled receptor (GPCR) agonists such as angiotensin II, phenylephrine, and others. Diacylglycerol functions as a potent activator of protein kinase C (PKC) and is catalyzed by diacylglycerol kinase (DGK) to form phosphatidic acid and inactivated. However, the functional roles of DGK have not been previously examined in the heart. We hypothesized that DGK might prevent GPCR agonist–induced activation of diacylglycerol downstream signaling cascades and subsequent cardiac hypertrophy.

Methods and Results—To test this hypothesis, we generated transgenic (DGKζ-TG) mice with cardiac-specific overexpression of DGKζ. There were no differences in heart size and heart weight between DGKζ-TG and wild-type littermate mice. The left ventricular function was normal in DGKζ-TG mice. Continuous administration of subpressor doses of angiotensin II and phenylephrine caused PKC translocation, gene induction of atrial natriuretic factor, and subsequent cardiac hypertrophy in WT mice. However, in DGKζ-TG mice, neither translocation of PKC nor upregulation of atrial natriuretic factor gene expression was observed after angiotensin II and phenylephrine infusion. Furthermore, in DGKζ-TG mice, angiotensin II and phenylephrine failed to increase cross-sectional cardiomyocyte areas and heart to body weight ratios. Phenylephrine-induced increases in myocardial diacylglycerol levels were completely blocked in DGKζ-TG mouse hearts, suggesting that DGKζ regulated PKC activity by controlling cellular diacylglycerol levels.

Conclusions—These results demonstrated the first evidence that DGKζ negatively regulated the hypertrophic signaling cascade and resultant cardiac hypertrophy in response to GPCR agonists without detectable adverse effects in in vivo hearts. (***Circulation.*** **2006;113:60-66.)**

Key Words: angiotensin ■ hypertrophy ■ enzymes ■ signal transduction

Cardiac hypertrophy is an initially adaptive response in several forms of cardiac disease, whereas sustained hypertrophy is a powerful independent risk factor for cardiac morbidity and mortality.[1] Therefore, to identify the critical molecular mechanisms involved in cardiac hypertrophy is an important challenge of cardiovascular biology and medicine. Multiple lines of experimental and clinical evidence have suggested the importance of the Gqα-phosphoinositide signaling system in the development of pathological cardiac hypertrophy and heart failure.[2–6] Gqα protein–coupled receptor (GPCR) agonists such as angiotensin II,[7] endothelin-1,[8] and phenylephrine[9] activate phospholipase C–mediated hydrolysis of phosphatidylinositol 4,5-bisphosphate, which produces inositol 1,4,5-trisphosphate and diacylglycerol (DAG). DAG functions as a potent activator of protein kinase C (PKC). The binding of DAG to the C1 domain of PKC induces an active conformation, and activated PKC regulates a variety of cellular functions including cell growth and differentiation. We and others have previously demonstrated that PKC plays an important role in the development and progression of cardiac hypertrophy.[10–12]

One major route for terminating DAG signaling is thought to be its phosphorylation and inactivation by DAG kinase (DGK), producing phosphatidic acid.[13–16] A previous study

Received July 20, 2004; de novo received May 10, 2005; revision received October 6, 2005; accepted October 17, 2005.

From the First Department of Internal Medicine (T.A., Y.T., H.T., T.S., T.N., Y.K., R.S., N.N., I.K.), Research Laboratory for Molecular Genetics (O.N.), Department of Cardiovascular Pharmacology (K.N., M.E.), and Department of Anatomy and Cell Biology (K.G.), Yamagata University School of Medicine, Yamagata, Japan; Center for Cardiovascular Research, University of Rochester, Rochester, NY (J.A.); and Department of Medicine, Case Western Reserve University, Cleveland, Ohio (R.A.W.).

Reprint requests to Yasuchika Takeishi, MD, First Department of Internal Medicine, Yamagata University School of Medicine, 2-2-2 Iida-Nishi, Yamagata, Japan 990-9585. E-mail takeishi@med.id.yamagata-u.ac.jp

Circulation is available at http://www.circulationaha.org

DOI: 10.1161/CIRCULATIONAHA.105.560771

has shown that of the α, ε, and ζ isoforms of DGK expressed in the myocardium, DGKζ is the predominant isoform.[17] We have recently demonstrated using cultured rat neonatal cardiomyocytes that DGKζ blocks endothelin-1–induced activation of PKC, extracellular signal–regulated kinase (ERK), and activator protein-1.[18] DGKζ also inhibits gene induction of atrial natriuretic factor (ANF), increases in protein synthesis, and resultant cardiomyocyte hypertrophy in response to endothelin-1 in neonatal cardiomyocytes. However, the in vivo role of DGKζ has not been previously investigated in the heart.[19]

We hypothesized that DGKζ may act as a negative regulator for GPCR agonist–induced activation of the DAG-PKC signaling cascade and subsequent cardiac hypertrophy in vivo. To test this hypothesis, we generated transgenic mice with cardiac-specific overexpression of DGKζ using an α-myosin heavy chain (MHC) promoter. We examined the functional role of DGKζ to interfere with hypertrophic responses by GPCR agonists such as angiotensin II and phenylephrine in transgenic mouse hearts.

Methods

Generation of DGKζ Transgenic Mice

All experimental procedures were performed according to the animal welfare regulations of Yamagata University School of Medicine, and the study protocol was approved by the Animal Subjects Committee of Yamagata University School of Medicine. The investigation conformed to the *Guide for the Care and Use of Laboratory Animals* published by the US National Institutes of Health.

Transgenic mice with cardiac-specific overexpression of DGKζ (DGKζ-TG) were created in Yamagata University by standard techniques.[10,12,20] Briefly, a 5.5-kb fragment of murine α-MHC gene promoter (a kind gift from Dr J. Robbins, Children's Hospital Research Foundation, Cincinnati, Ohio) and 3.4-kb rat DGKζ cDNA[13] were subcloned into pBsIISK(+) plasmids. The plasmid was digested with *SpeI* to generate a 9.5-kb DNA fragment composed of the α-MHC gene promoter, DGKζ cDNA, and a poly A tail of the human growth hormone, as illustrated in Figure 1A. We microinjected the construct into the pronuclei of single-cell fertilized mouse embryos to generate transgenic mice as previously described.[10,12,20] To detect the exogenous DGKζ gene, genomic DNA was extracted from the tail tissues of 3- to 4-week-old pups, and polymerase chain reaction (PCR) was performed with one primer specific for the α-MHC gene promoter and another primer specific for the DGKζ, as shown in Figure 1A.

DGK Activity

DGK activity in the left ventricle was measured by octyl glucoside mixed-micelle assay as described previously.[21,22] The 1,2-dioleoyl-*sn*-glycerol (18:1/18:1 DAG) and 1-stearoyl-2- linoleoyl-*sn*-glycerol (18:0/18:2 DAG) were used as substrates for kinase assays. Phosphatidic acid separated by thin layer chromatography was scraped and counted by liquid scintillation.[21,22]

Western Blotting

Total protein was extracted from the left ventricle with ice-cold lysis buffer as described previously.[23–25] Protein concentration of myocardial samples was carefully determined by the protein assay, and equal amounts of protein extracts were loaded on each gel lane. To ensure equivalent protein loading and quantitative transfer efficiency of proteins, membranes were stained with Ponceau S before incubating with primary antibodies. Western blotting was performed as reported previously, and DGKζ protein levels in TG mice were expressed as fold increase over wild-type (WT) mice. Membrane and cytosolic fractions were also prepared from left ventricular myocardium as previously reported.[10,12,25] Membrane/cytosol ratios of immunoreactivity with the use of isoform-specific antibodies (mouse monoclonal anti-PKCα, β, δ, and ε; Santa Cruz Biotechnology, Inc, Santa Cruz, Calif) were used as indices for the extent of translocation of PKC isoforms.[10,12,25]

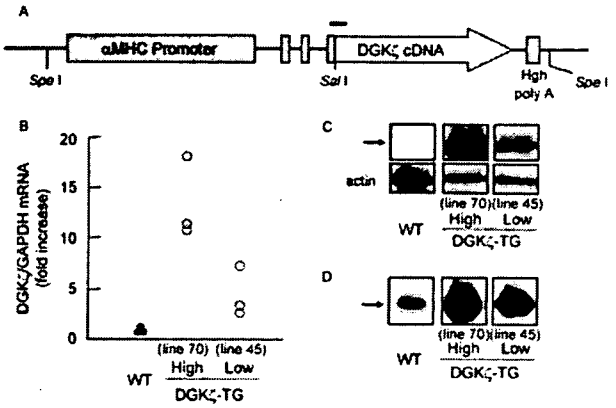

Figure 1. A, Diagram of the transgene construct used for the generation of DGKζ-TG mice. The construct contains the α-MHC gene promoter, the full-length rat DGKζ cDNA clone, and a human growth hormone (Hgh) polyadenylylation sequence. The solid line indicates the region amplified by PCR for genotyping. B, Quantitative analysis of DGKζ mRNA expression in the left ventricle of DGKζ-TG and WT mice. Left ventricular myocardium of 8-week-old mice was examined by real-time PCR analysis and normalized with the use of GAPDH mRNA. Data are reported as fold increase over WT and obtained from 3 mice for each. C, Representative Western blot analysis of DGKζ protein from the left ventricle of DGKζ-TG-High, DGKζ-TG-Low, and WT mice. D, Representative autoradiograms of DGK assay of DGKζ-TG-High, DGKζ-TG-Low, and WT mice.

Extraction of Total RNA and Real-time Reverse Transcriptase–PCR

Total RNAs were extracted from the left ventricle, and first-strand cDNA was synthesized as previously described.[26,27] To examine mRNA levels of DGKζ and ANF quantitatively, real-time reverse transcriptase–PCR (RT-PCR) amplification was performed.[18] Amplification was performed with the use of LightCycler and analyzed with the use of LightCycler Software Version 3.5 (Roche Diagnostics Japan). Standard curves of DGKζ and ANF were generated by full sequence plasmid of known concentrations. Gene expression was normalized to glyceraldehyde 3-phosphate dehydrogenase (GAPDH) and expressed as fold increase over WT mice. Primers were designed on the basis of GenBank sequences (DGKζ, BC049228; ANF, K02781; and GAPDH, NM_001001303).

Isolated Cardiomyocyte Function and Ca^{2+} Transient

Ventricular myocytes were isolated from hearts from WT mice and mouse lines with the high expression of transgene mRNA (DGKζ-TG-High), and cardiomyocyte mechanical properties were examined with the use of a computerized edge-detection analyzer as previously reported.[28] Cells were paced at 0.5 Hz throughout the experiments. Same isolated cells were used for measurements of cytosolic free Ca^{2+} by indo-1 with a previously described method.[28] Data from at least 5 to 6 cardiomyocytes were averaged for each mouse heart, and the statistical analysis was performed on the basis of the number of hearts studied (n=6 for each group).

Histological Examinations

Coronary arteries were retrogradely flushed with saline, and the heart was fixed with 4% paraformaldehyde at 4°C for 24 hours and then embedded in paraffin.[26,27] Three sections were stained with

hematoxylin-eosin or elastica Goldner stain. Transverse sections were captured digitally, and cardiomyocyte cross-sectional area was measured with the use of a Scion imaging system (Scion Corporation).[29] At least 300 cardiomyocytes were examined in each heart, and the data were averaged.

Hemodynamic Measurements and Echocardiography

Heart rate (bpm) and blood pressure (mm Hg) were determined with animals in the conscious state with the use of a computerized tail-cuff manometer, MK-1030 (Muromachi Kikai Co, Ltd), as reported previously.[12] Echocardiography was performed as described previously[26,27] with an FFsonic 8900 (Fukuda Denshi Co) equipped with a 13-MHz phased-array transducer. Left ventricular wall thickness and internal dimensions at end-systole and end-diastole were measured digitally on the M-mode tracings and averaged for 3 cardiac cycles. Left ventricular fractional shortening was calculated as previously reported.[26,27]

Lipid Extraction and Measurements of Myocardial DAG Levels

Myocardial lipid extract was prepared from the left ventricle, and DAG levels were measured as previously reported.[30] Briefly, with the use of the DAG within myocardial lipid extract as substrate and with the use of [γ-^{32}P]ATP, myocardial DAG level was quantified by production of [^{32}P]phosphatidic acid. Lipid extract was solubilized in 50 μL of 0.6% (wt/vol) Triton X/288 μmol/L phosphatidylserine. The reaction mixture contained 0.3% (wt/vol) Triton X, 144 μmol/L phosphatidylserine, 50 mmol/L imidazole/HCl, pH 6.6, 50 mmol/L NaCl, 12.5 mmol/L $MgCl_2$, 1 mmol/L EGTA, 10 mmol/L dithiothreitol, 0.5 mmol/L ATP (1 μCi of [γ-^{32}P]ATP), and 5 m-unit of DGK (*Escherichia coli*). After 30 minutes of incubation, the reaction was terminated, and the radiolabeled product was separated by TLC on silica plates. The [^{32}P]phosphatidic acid was identified by autoradiography. Silica corresponding to phosphatidic acid was scraped and counted by liquid scintillation counting.[30]

Subcutaneous Implantation of Osmotic Minipump

A subpressor dose of angiotensin II (100 ng/kg per minute) or phenylephrine (20 mg/kg per day) dissolved in saline or saline alone (control) was continuously infused into mice subcutaneously via an osmotic minipump (ALZET Osmotic Pumps, DURECT Corporation) for 14 or 3 days, respectively.[2,3,31,32] Heart rate and blood pressure were measured before and after subcutaneous infusion of angiotensin II or phenylephrine.

Statistical Analysis

All values are reported as mean±SD. Comparisons of hemodynamic data and gravimetric and echocardiographic measurements at basal conditions among WT, DGKζ-TG-High, and DGKζ-TG-Low mice were made by the Kruskal-Wallis test. Isolated cardiomyocyte mechanical properties and calcium transient data between WT and DGKζ-TG-High mice were compared by the Mann-Whitney *U* test. Effects of angiotensin II and phenylephrine on body weight, blood pressure, heart rate, heart weight, left ventricular weight, PKC translocation, DAG level, ANF expression, and cardiomyocyte surface area in animal groups were compared by 2-way ANOVA followed by multiple comparisons with the Bonferroni test. Probability values of <0.05 were considered statistically significant.

Results

Generation of DGKζ Transgenic Mice

After microinjection and embryo implantation, 2 lines of transgenic mice (lines 70 and 45) were successfully established. Figure 1B shows the real-time PCR results of DGKζ in the left ventricle of TG and WT mice. Heterozygous mouse lines with the high expression of transgene mRNA (DGKζ-TG-High) and the low expression of transgene mRNA (DGKζ-TG-Low) in the left ventricle were characterized in detail in the following experiments. RNA was extracted from brain, heart, lungs, liver, kidney, spleen, intestine, and skeletal muscle tissues of DGKζ-TG mice, and cardiac-specific expression of transgene was confirmed by RT-PCR (data not shown). Protein levels of DGKζ were augmented 21- and 5.5-fold in DGKζ-TG-High and DGKζ-TG-Low hearts compared with control WT littermates, respectively (Figure 1C). Additionally, we confirmed that kinase activities of DGK in the heart were also augmented in both DGKζ-TG mouse lines (Figure 1D). No neonatal and adult deaths were observed in DGKζ-TG mice.

TABLE 1. Gravimetric Data and In Vivo Cardiac Function of DGKζ-TG Mice at Basal Condition

	WT	DGKζ-TG-High	DGKζ-TG-Low
BW, g	22.6±1.1	21.7±2.8	23.5±3.8
BP, mm Hg	96±13	99±6	95±7
HR, bpm	673±52	643±71	650±68
HW, mg	117±9	122±16	122±18
LVW, mg	77±6	78±15	80±14
HW/BW, mg/g	4.92±0.24	5.07±0.41	4.94±0.33
LVW/BW, mg/g	3.25±0.14	3.22±0.44	3.24±0.38
Echocardiography			
LVEDD, mm	3.31±0.17	3.21±0.17	3.24±0.28
LVESD, mm	1.60±0.15	1.50±0.19	1.45±0.15
LVFS, %	52±4	53±5	53±5
IVS, mm	0.64±0.07	0.64±0.05	0.63±0.05
PW, mm	0.66±0.05	0.65±0.05	0.65±0.05

Data were analyzed by the Kruskal-Wallis test and are reported as mean±SD (n=8). BW indicates body weight; BP, blood pressure; HR, heart rate; HW, heart weight; LVW, left ventricular weight; LVEDD, left ventricular end-diastolic dimension; LVESD, left ventricular end-systolic dimension; LVFS, left ventricular fractional shortening; IVS, interventricular septum; and PW, posterior wall.

Gravimetric Data, Cardiac Function, and Isolated Cardiomyocyte Mechanical Properties of DGKζ-TG Mice at Basal Condition

To characterize mouse phenotype, all experiments were performed with age- and sex-matched (8- to 10-week-old) DGKζ-TG and WT littermate mice. Body weight, blood pressure, and heart rate were similar between DGKζ-TG and WT mice (Table 1). There was no evidence of fibrosis on microscopic examinations of multiple histological sections (data not shown). The absolute heart weight, ratio of heart to body weight, and ratio of the left ventricle to body weight were not different between DGKζ-TG and WT mice (Table 1). Echocardiography demonstrated that cardiac dimensions, wall thickness, and fractional shortening were normal in DGKζ-TG mice, as shown in Table 1. Isolated cardiomyocyte mechanical properties and Ca^{2+} transients were examined with the use of 6 WT mice and 6 DGKζ-TG-High mice. Cell shortening (4.10±0.47% versus 4.71±0.49%), time to peak shortening (52±4 versus 54±6 ms), and time to 80% relaxation (105±17 versus 89±17 ms) were not different between

TABLE 2. Changes in Hemodynamic and Gravimetric Parameters in WT and DGKζ-TG Mice After Angiotensin II or Phenylephrine Infusion

	WT			DGKζ-TG-High			DGKζ-TG-Low		
	Saline	Ang II (14 d)	PE (3 d)	Saline	Ang II (14 d)	PE (3 d)	Saline	Ang II (14 d)	PE (3 d)
BW, g	21.5±2.1	23.5±2.9	23.9±2.5	24.1±3.4	22.0±3.0	21.7±2.8	25.8±3.5	23.8±4.0	24.0±1.9
BP, mm Hg	99±14	101±14	102±6	99±7	105±13	110±6	96±8	94±8	107±17
HR, bpm	665±47	663±38	641±29	632±99	631±41	624±61	632±70	663±33	670±61
HW/BW, mg/g	4.96±0.29	5.51±0.27*	5.76±0.81*	5.03±0.23	5.07±0.11†	4.95±0.39§	4.93±0.34	4.98±0.57†	5.19±0.37‡
LVW/BW, mg/g	3.22±0.20	3.98±0.18*	3.91±0.63*	3.21±0.38	3.34±0.20†	3.38±0.38§	3.24±0.36	3.22±0.34†	3.38±0.41‡

Data were analyzed by 2-way ANOVA followed by multiple comparisons with the Bonferroni test and are presented as mean±SD (n=6). Ang II indicates angiotensin II; PE, phenylephrine; BW, body weight; BP, blood pressure; HR, heart rate; HW, heart weight; and LVW, left ventricular weight.
*P<0.01 vs saline-infused WT mice; †P<0.01 vs Ang II–infused WT mice; ‡P<0.05 and §P<0.01 vs PE-infused WT mice.

DGKζ-TG-High and WT mice. The amplitude of the Ca^{2+} signal (0.084±0.011 versus 0.077±0.007) and half-life decay of the Ca^{2+} signal (156±13 versus 162±13 ms) were also same between DGKζ-TG-High and WT mice.

Effects of DGKζ on GPCR Agonist–Induced Activation of DAG-PKC Signaling

DGKζ-TG and WT mice were assessed with respect to their susceptibility to hypertrophic response to subpressor doses of subcutaneous angiotensin II[2,3] and phenylephrine[31,32] administration. No significant changes in body weight, heart rate, and blood pressure were observed between WT and DGKζ-TG mice after subcutaneous infusion of angiotensin II or phenylephrine, as shown in Table 2.

In the present study there were no significant changes in total protein abundance of PKC isoforms after angiotensin II or phenylephrine infusion (data not shown). We have previously demonstrated angiotensin II–induced translocation of PKC isoforms through pathways involving phospholipase C in the guinea pig ex vivo heart.[5] As shown in Figure 2, the membrane-associated immunoreactivities of PKCα and PKCε, but not PKCβ and PKCδ, were significantly increased in angiotensin II–treated WT mice compared with saline-infused WT mice (P<0.05). However, angiotensin II–induced translocation of PKCα and PKCε was blocked in both DGKζ-TG-High and DGKζ-TG-Low mice (P<0.05 versus angiotensin II–infused WT mice).

Next, we examined effects of another GPCR agonist, phenylephrine, in TGKζ-TG mice. Phenylephrine induced translocation of the PKCε isoform (P<0.01), but not α, β, and δ isoforms, in WT mouse hearts, as shown in Figure 3. However, in both DGKζ-TG-High and DGKζ-TG-Low mice, translocation of the PKCε by phenylephrine was completely blocked (P<0.01 versus phenylephrine-infused WT mice). These data suggested that DGKζ had an inhibitory effect on GPCR agonist–induced translocation of PKC isoforms in in vivo mouse hearts.

Lipid extracts were then prepared from the left ventricular myocardium, and we quantified myocardial DAG levels in WT and DGKζ-TG-High mouse hearts (n=6 for each group). At basal condition, DAG levels were similar between WT and DGKζ-TG-High mice (51±15 versus 66±18 pmol/mg tissue). In WT mouse hearts, myocardial DAG level increased significantly after continuous administration of phenylephrine for 3 days (from 51±15 to 103±27 pmol/mg tissue; P<0.001). On the other hand, this effect of phenylephrine on myocardial DAG levels was completely suppressed in DGKζ-TG-High mouse hearts (from 66±18 to 34±7 pmol/mg tissue; P=NS). These data suggest that DGKζ regulates PKC activity by controlling cellular DAG levels.

Effects of DGKζ on Hypertrophic Programs in Response to GPCR Agonists

Ventricular hypertrophy induced by continuous infusion of angiotensin II or phenylephrine is accompanied by the induction of several specific genes such as ANF.[2,18] As shown in Figure 4, the mRNA expression of ANF was increased in WT mice given angiotensin II and phenylephrine compared with saline-infused WT mice (P<0.01). However, in DGKζ-TG-High and DGKζ-TG-Low mice, angiotensin II failed to cause gene induction of ANF (P<0.01). Phenylephrine-induced ANF gene induction was significantly blocked in DGKζ-TG-High mice (P<0.01), but this inhibitory effect was not

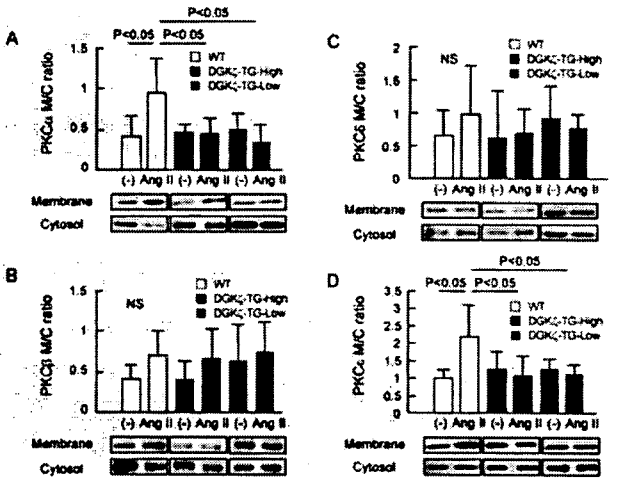

Figure 2. Translocation of PKCα (A), PKCβ (B), PKCδ (C), and PKCε (D) in DGKζ-TG-High, DGKζ-TG-Low, and WT mice in response to angiotensin II (Ang II). A subpressor dose of angiotensin II (100 ng/kg per minute) was continuously infused with an osmotic minipump for 14 days.[2,3] Membrane/cytosol (M/C) ratio of immunoreactivity was used as an index of PKC activation. Data were analyzed by 2-way ANOVA followed by multiple comparisons with the Bonferroni test and are reported as mean±SD obtained from 6 to 7 mice for each group.

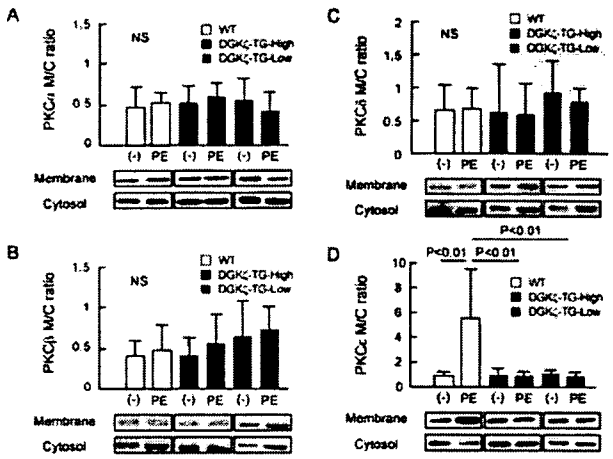

Figure 3. Translocation of PKCα (A), PKCβ (B), PKCδ (C), and PKCϵ (D) and in DGKζ-TG-High, DGKζ-TG-Low, and WT mice in response to phenylephrine (PE). A dose of phenylephrine (20 mg/kg per day) was infused into mice subcutaneously via an osmotic minipump for 3 days.[31,32] Membrane/cytosol (M/C) ratio of immunoreactivity was used as an index of PKC activation. Data were analyzed by 2-way ANOVA followed by multiple comparisons with the Bonferroni test and are reported as mean±SD obtained from 6 to 7 mice for each group.

statistically significant in DGKζ-TG-Low mice (P=0.0704). These data suggested that DGKζ blocked hypertrophic gene induction by angiotensin II and phenylephrine in in vivo mouse hearts.

As shown in Table 2, heart weight and left ventricular weight corrected for body weight were not significantly different between saline-infused WT and saline-infused DGKζ-TG mice. Subcutaneous infusion of angiotensin II and phenylephrine caused significant increases in the ratio of heart to body weight and ratio of the left ventricle to body weight in WT mice (P<0.01). However, in both DGKζ-TG-High and DGKζ-TG-Low mice, neither angiotensin II nor phenylephrine produced increases in the ratio of heart to body weight and ratio of the left ventricle to body weight (Table 2).

Microscopic observations revealed that no significant difference in cardiomyocyte cross-sectional area was seen between saline-infused WT and saline-infused DGKζ-TG mice

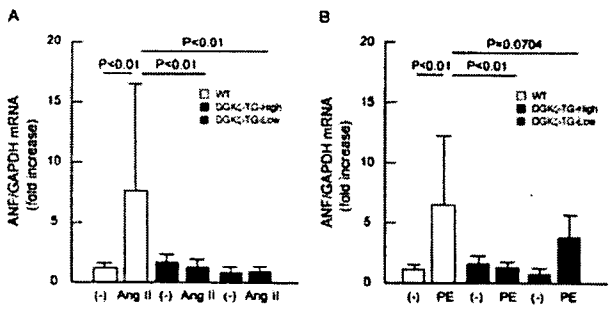

Figure 4. Cardiac ANF gene expressions in DGKζ-TG-High, DGKζ-TG-Low, and WT mice in response to angiotensin II (Ang II) (A) and phenylephrine (PE) (B). Mean value in saline-infused WT mice is presented as 1.0. Data were analyzed by 2-way ANOVA followed by multiple comparisons with the Bonferroni test. Data reported are mean±SD obtained from 6 to 8 mice for each group.

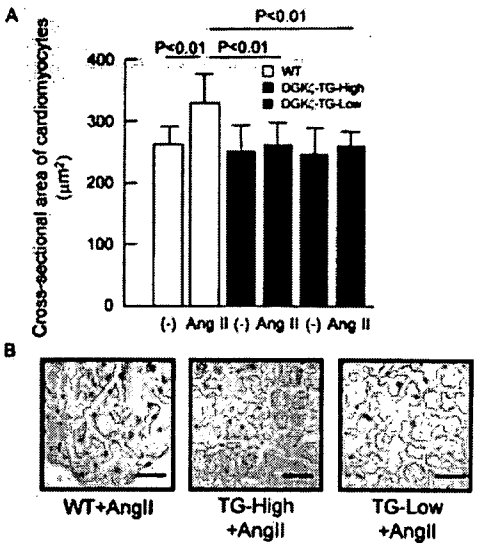

Figure 5. Histological analysis in DGKζ-TG-High, DGKζ-TG-Low, and WT mice after angiotensin II (AngII) infusion. Bottom panels show representative images of hematoxylin-eosin micrographs of cardiomyocyte cross sections. (Magnification ×200, bar=20 μm). Top bar graph shows quantitative analysis of cardiomyocyte cross-sectional area from the left ventricle. Data were analyzed by 2-way ANOVA followed by multiple comparisons with the Bonferroni test. Data reported are mean±SD obtained from 7 mice for each group.

(Figures 5 and 6). In WT mice, cardiomyocyte cross-sectional area was significantly increased by angiotensin II and phenylephrine infusion (P<0.01 and P<0.05, respectively). However, in both DGKζ-TG-High and DGKζ-TG-Low mice, neither angiotensin II nor phenylephrine caused increases in

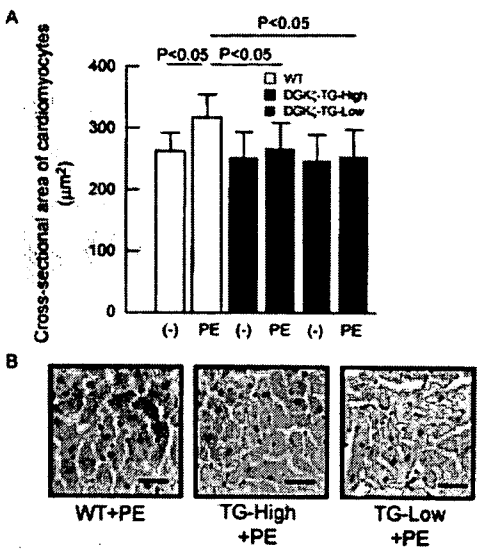

Figure 6. Histological analysis in DGKζ-TG-High, DGKζ-TG-Low, and WT mice after phenylephrine (PE) infusion. Bottom panels show representative images of hematoxylin-eosin micrographs of cardiomyocyte cross sections. (magnification ×200, bar=20 μm). Top bar graph shows quantitative analysis of cardiomyocyte cross-sectional area from the left ventricle. Data were analyzed by 2-way ANOVA followed by multiple comparisons with the Bonferroni test. Data are reported as mean±SD obtained from 7 mice for each group.

cardiomyocyte cross-sectional area ($P<0.01$ versus angiotensin II–infused WT and $P<0.05$ versus phenylephrine-infused WT mice). Obvious fibrosis in the myocardium was not observed in DGKζ-TG and WT mice given angiotensin II or phenylephrine (data not shown). Taken together, these data clearly demonstrated that DGKζ might interfere with GPCR agonist–induced cardiac hypertrophy.

Discussion

This is the first report characterizing a functional role of DGKζ in the in vivo mouse heart. Molecular, gravimetric, and morphological analyses clearly showed that cardiac-specific overexpression of DGKζ abrogated cardiac hypertrophy in response to GPCR agonists such as angiotensin II and phenylephrine by regulating the DAG-PKC signaling in transgenic mouse hearts.

DGKζ-TG mice were indistinguishable in appearance from WT mice, and no baseline cardiac effects were observed in physiological or histological analyses. In addition, we found that isolated cardiomyocyte function and in vivo cardiac function evaluated by echocardiography were normal in DGKζ-TG mice. Blood pressure and heart rate after subcutaneous infusion of angiotensin II and phenylephrine were not different among DGKζ-TG-High, DGKζ-TG-Low, and WT mice, indicating that the overexpression of DGKζ does not affect hemodynamic regulations in response to angiotensin II and phenylephrine. Consistent with previous works,[2,3,31,32] the hypertrophic response in this study occurred independently of the hemodynamic effects of angiotensin II and phenylephrine because systemic blood pressure was not elevated after infusion.

Previous studies in human heart failure and animal models of heart failure have clearly demonstrated that activation of PKC isoforms plays a critical role in the development of cardiac hypertrophy and progression to heart failure.[5,6,10–12] GPCR agonists increase production of DAG, resulting in sustained PKC activation in the cardiomyocyte.[7,33] DGK is an enzyme that is responsible for controlling the cellular levels of DAG by converting it to phosphatidic acid, and thus is thought to be acting as an endogenous regulator of PKC activity. Continuous infusion of phenylephrine for 3 days increased myocardial DAG levels in WT mice, but this effect was completely abolished by overexpression of DGKζ. These data suggest that DGKζ regulates PKC activity by controlling cellular DAG levels.

Phosphatidic acid is yielded not only by DGK but also by the action of phospholipase D. Phospholipase D hydrolyzes phosphatidylcholine to form phosphatidic acid, and phosphatidic acid itself also has signaling function, stimulates DNA synthesis, and modulates activity of several enzymes, including phosphatidylinositol 5-kinases, ERK, and others.[34] However, because the bulk of the signaling pool of phosphatidic acid is mainly derived from the action of phospholipase D in cardiomyocytes,[35] overexpression of DGKζ may not affect phosphatidic acid pool and its signaling function. We previously demonstrated that activation of downstream ERK and protein synthesis by endothelin-1 were abolished by DGKζ in isolated neonatal rat cardiomyocytes.[18] These results suggested the importance of inhibiting the DAG-PKC signaling pathway by DGKζ to prevent cardiomyocyte hypertrophy.

The in vitro studies have reported that DGK isoforms modulate the DAG-PKC signaling in several types of cells.[36,37] In particular, Luo et al[38] have recently showed that DGKζ spatially regulates PKCα activity by attenuating local accumulation of DAG in HEK293 cells. It has been reported that the DGKε isoform reduces cellular DAG levels in aortic endothelial cells.[36] We have recently found that adenovirus-mediated overexpression of the DGKζ isoform blocked endothelin-1–induced activation of the DAG-PKC signaling and resultant cardiomyocyte hypertrophy in cultured rat neonatal cardiomyocytes.[18] To further elucidate these issues obtained from in vitro studies, isoform-specific regulation of DGK in an in vivo study with the use of a transgenic approach, as we employed in the present study, is necessary. In our present study, angiotensin II– and phenylephrine-induced translocation of PKC was blocked in DGKζ-TG mice (Figures 2 and 3). These data suggest that DGKζ has an inhibitory effect on PKC translocation, which depends on kinase activity, in the left ventricular myocardium. Furthermore, angiotensin II– and phenylephrine-induced hypertrophic programs determined by gene induction of ANF, increases in heart weight, and enlargements of cardiomyocyte surface area were abolished in DGKζ-TG mice (Table 2 and Figures 4 to 6). These data suggest that DGKζ functions as a negative regulator of the DAG-PKC signaling and prevents subsequent cardiomyocyte hypertrophy. Because this study used only the overexpression approach, future experiments of a loss of DGK function with the use of knockout mice are necessary to elucidate further the role of DGKζ in signaling cascade in vivo.

In conclusion, our study provides the first in vivo evidence that DGKζ blocks cardiac hypertrophy in response to GPCR agonists by regulating DAG-PKC signaling. Further studies will be necessary to examine whether and to what extent DGKζ may prevent pressure overload–induced cardiac hypertrophy.

Acknowledgments

This study was supported in part by a grant-in-aid for scientific research (No. 17590702) from the Ministry of Education, Science, Sports, and Culture, Japan; a grant-in-aid from the 21st Century Center of Excellence (COE) program of the Japan Society for the Promotion of Science; and grants from the Japan Heart Foundation, the Mochida Memorial Foundation, and Takeda Science Foundation. We thank Shuku Takahashi and Sachi Adachi for their excellent technical assistance.

Disclosures

None.

References

1. Levy D, Garrison RJ, Savage DD, Kannel WB, Castelli WP. Prognostic implications of echocardiographically determined left ventricular mass in the Framingham Heart Study. *N Engl J Med.* 1990;322:1561–1566.
2. Harada K, Komuro I, Shiojima I, Hayashi D, Kudoh S, Mizuno T, Kijima K, Matsubara H, Sugaya T, Murakami K, Yazaki Y. Pressure overload induces cardiac hypertrophy in angiotensin II type 1A receptor knockout mice. *Circulation.* 1998;97:1952–1959.
3. Schultz Jel J, Witt SA, Glascock BJ, Nieman ML, Reiser PJ, Nix SL, Kimball TR, Doetschman T. TGF-β1 mediates the hypertrophic cardio-

myocyte growth induced by angiotensin II. *J Clin Invest.* 2002;109: 787–796.
4. Izumiya Y, Kim S, Izumi Y, Yoshida K, Yoshiyama M, Matsuzawa A, Ichijo H, Iwao H. Apoptosis signal-regulating kinase 1 plays a pivotal role in angiotensin II–induced cardiac hypertrophy and remodeling. *Circ Res.* 2003;93:874–883.
5. Takeishi Y, Jalili T, Ball NA, Walsh RA. Responses of cardiac protein kinase C isoforms to distinct pathological stimuli are differentially regulated. *Circ Res.* 1999;85:264–271.
6. Hunter JJ, Chien KR. Signaling pathways for cardiac hypertrophy and failure. *N Engl J Med.* 1999;341:1276–1283.
7. Sadoshima J, Izumo S. Signal transduction pathways of angiotensin II–induced c-fos gene expression in cardiac myocytes in vitro: roles of phospholipid-derived second messengers. *Circ Res.* 1993;73:424–438.
8. Shubeita HE, McDonough PM, Harris AN, Knowlton KU, Glembotski CC, Brown JH, Chien KR. Endothelin induction of inositol phospholipid hydrolysis, sarcomere assembly, and cardiac gene expression in ventricular myocytes: a paracrine mechanism for myocardial cell hypertrophy. *J Biol Chem.* 1990;265:20555–20562.
9. Otani H, Otani H, Das DK. α1-Adrenoceptor-mediated phosphoinositide breakdown and inotropic response in rat left ventricular papillary muscles. *Circ Res.* 1988;62:8–17.
10. Takeishi Y, Chu G, Kirkpatrick DL, Wakasaki H, Li Z, Kranias EG, King GL, Walsh RA. In vivo phosphorylation of cardiac troponin I by PKCβ2 decreases cardiomyocyte calcium responsiveness and contractility in transgenic mouse heart. *J Clin Invest.* 1998;102:72–78.
11. Bowling N, Walsh RA, Song G, Estridge T, Sandusky GE, Fouts RL, Mintze K, Pickard T, Roden R, Bristow MR, Sabbah HN, Mizrahi JL, Gromo G, King GL, Vlahos CJ. Increased protein kinase C activity and expression of Ca^{2+}-sensitive isoforms in the failing human heart. *Circulation.* 1999;99:384–391.
12. Takeishi Y, Ping P, Bolli R, Kirkpatrick DL, Hoit BD, Walsh RA. Transgenic overexpression of constitutively active protein kinase C-ϵ causes concentric cardiac hypertrophy. *Circ Res.* 2000;86:1218–1223.
13. Goto K, Kondo H. A 104-kDa diacylglycerol kinase containing ankyrin-like repeats localizes in the cell nucleus. *Proc Natl Acad Sci U S A.* 1996;93:11196–11201.
14. Topham MK, Bunting M, Zimmerman GA, McIntyre TM, Blackshear PJ, Prescott SM. Protein kinase C regulates the nuclear localization of diacylglycerol kinase-ζ. *Nature.* 1998;394:697–700.
15. Topham MK, Prescott SM. Mammalian diacylglycerol kinases, a family of lipid kinases with signaling functions. *J Biol Chem.* 1999;274: 11447–11450.
16. Goto K, Kondo H. Diacylglycerol kinase in the central nervous system: molecular heterogeneity and gene expression. *Chem Phys Lipids.* 1999; 98:109–117.
17. Takeda M, Kagaya Y, Takahashi J, Sugie T, Ohta J, Watanabe J, Shirato K, Kondo H, Goto K. Gene expression and in situ localization of diacylglycerol kinase isozymes in normal and infarcted rat hearts: effects of captopril treatment. *Circ Res.* 2001;89:265–272.
18. Takahashi H, Takeishi Y, Seidler T, Arimoto T, Akiyama H, Koyama Y, Shishido T, Tsunoda Y, Niizeki T, Hozumi Y, Abe J, Hasenfuss G, Goto K, Kubota I. Adenovirus-mediated overexpression of diacylglycerol kinase ζ inhibits endothelin-1–induced cardiomyocyte hypertrophy. *Circulation.* 2005;111:1510–1516.
19. Arimoto T, Takahashi H, Shishido T, Niizeki T, Koyama Y, Nakajima O, Goto K, Takeishi Y. Cardiac-specific overexpression of diacylglycerol ζ prevents angiotensin II–induced cardiac hypertrophy in transgenic mice. *Circulation.* 2004;110:III-226. (Abstract)
20. Gordon JW, Scangos GA, Plotkin DJ, Barbosa JA, Ruddle FH. Genetic transformation of mouse embryos by microinjection of purified DNA. *Proc Natl Acad Sci U S A.* 1980;77:7380–7384.
21. Goto K, Kondo H. Molecular cloning and expression of a 90-kDa diacylglycerol kinase that predominantly localizes in neurons. *Proc Natl Acad Sci U S A.* 1993;90:7598–7602.
22. Goto K, Funayama M, Kondo H. Cloning and expression of a cytoskeleton-associated diacylglycerol kinase that is dominantly expressed in cerebellum. *Proc Natl Acad Sci U S A.* 1994;91: 13042–13046.
23. Takeishi Y, Abe J, Lee JD, Kawakatsu H, Walsh RA, Berk BC. Differential regulation of p90 ribosomal S6 kinase and big mitogen-activated protein kinase-1 by ischemia/reperfusion and oxidative stress in perfused guinea pig hearts. *Circ Res.* 1999;85:1164–1172.
24. Takeishi Y, Huang Q, Abe J, Glassman M, Che W, Lee JD, Kawakatsu H, Lawrence EG, Hoit BD, Berk BC, Walsh RA. Src and multiple MAP kinase activation in cardiac hypertrophy and congestive heart failure under chronic pressure-overload: comparison with acute mechanical stretch. *J Mol Cell Cardiol.* 2001;33:1637–1648.
25. Takahashi H, Takeishi Y, Miyamoto T, Shishido T, Arimoto T, Konta T, Miyashita T, Ito M, Kubota I. Protein kinase C and extracellular signal regulated kinase are involved in cardiac hypertrophy of rats with progressive renal injury. *Eur J Clin Invest.* 2004;34:85–93.
26. Shishido T, Nozaki N, Yamaguchi S, Shibata Y, Nitobe J, Miyamoto T, Takahashi H, Arimoto T, Maeda K, Yamakawa M, Takeuchi O, Akira S, Takeishi Y, Kubota I. Toll-like receptor-2 modulates ventricular remodeling after myocardial infarction. *Circulation.* 2003;108: 2905–2910.
27. Nozaki N, Shishido T, Takeishi Y, Kubota I. Modulation of doxorubicin-induced cardiac dysfunction in toll-like receptor-2 knockout mice. *Circulation.* 2004;110:2869–2874.
28. Kubota I, Tomoike H, Han X, Sakurai K, Endoh M. The Na^+-Ca^{2+} exchanger contributes to β-adrenoceptor mediated positive inotropy in mouse heart. *Jpn Heart J.* 2002;43:399–407.
29. Bendall JK, Cave AC, Heymes C, Gall N, Shah AM. Pivotal role of a gp91(phox)-containing NADPH oxidase in angiotensin II–induced cardiac hypertrophy in mice. *Circulation.* 2002;105:293–296.
30. Paterson A, Plevin R, Wakelam MJO. Accurate measurement of *sn*-1,2-diradyl-glycerol mass in cell lipid extracts. *Biochem J.* 1991;280: 829–836.
31. Asakura M, Kitakaze M, Takashima S, Liao Y, Ishikura F, Yoshinaka T, Ohmoto H, Node K, Yoshino K, Ishiguro H, Asanuma H, Sanada S, Matsumura Y, Takeda H, Beppu S, Tada M, Hori M, Higashiyama S. Cardiac hypertrophy is inhibited by antagonism of ADAM12 processing of HB-EGF: metalloproteinase inhibitors as a new therapy. *Nat Med.* 2002;8:35–40.
32. Roman BB, Geenen DL, Leitges M, Buttrick PM. PKC-beta is not necessary for cardiac hypertrophy. *Am J Physiol.* 2001;280:H2264–2270.
33. Ohanian J, Ollerenshaw J, Collins P, Heagerty A. Agonist-induced production of 1,2-diacylglycerol and phosphatidic acid in intact resistance arteries: evidence that accumulation of diacylglycerol is not a prerequisite for contraction. *J Biol Chem.* 1990;265:8921–8928.
34. Dhalla NS, Xu YJ, Sheu SS, Tappia PS, Panagia V. Phosphatidic acid: a potential signal transducer for cardiac hypertrophy. *J Mol Cell Cardiol.* 1997;29:2865–2871.
35. Exton JH. Phospholipase D: enzymology, mechanisms of regulation, and function. *Physiol Rev.* 1997;77:303–320.
36. Pettitt TR, Wakelam MJ. Diacylglycerol kinase ϵ, but not ζ, selectively removes polyunsaturated diacylglycerol, inducing altered protein kinase C distribution in vivo. *J Biol Chem.* 1999;274:36181–36186.
37. Verrier E, Wang L, Wadham C, Albanese N, Hahn C, Gamble JR, Chatterjee VK, Vadas MA, Xia P. PPARγ agonists ameliorate endothelial cell activation via inhibition of diacylglycerol-protein kinase C signaling pathway: role of diacylglycerol kinase. *Circ Res.* 2004;94:1515–1522.
38. Luo B, Prescott SM, Topham MK. Association of diacylglycerol kinase ζ with protein kinase C α: spatial regulation of diacylglycerol signaling. *J Cell Biol.* 2003;160:929–937.

Circ J 2007; **71:** 397–404

Resveratrol Ameliorates Experimental Autoimmune Myocarditis

Yuki Yoshida, MD; Tetsuo Shioi, MD; Tohru Izumi, MD

Background Myosin-induced autoimmune myocarditis of rats is a model of human dilated cardiomyopathy. Resveratrol is a natural polyphenol found in grapes and wine that is reported to have cardioprotective and immunomodulatory effects.

Methods and Results To examine the effect of resveratrol on myocarditis, vehicle or resveratrol (50 mg/kg per day) was administered to cardiac myosin immunized rats 1 day before the immunization. At 14 days after immunization, resveratrol had preserved cardiac function of myosin-immunized rats according to echocardiographic analysis. The heart weight/tibial length ratio of vehicle-treated myosin-immunized rats was increased by 1.8-fold compared with unimmunized rats, and resveratrol attenuated the heart weight increase. Resveratrol significantly decreased cellular infiltration, fibrosis, and expression of inflammatory cytokines in the myocardium. Expressions of antioxidant genes were increased in myosin-immunized hearts, and resveratrol decreased those expressions. Resveratrol also attenuated myocarditis 21 days after immunization. SIRT1, a potential effector of resveratrol, was increased in the myocardium of myosin-immunized rats compared with unimmunized rats. The SIRT1 protein was localized mainly in infiltrating mononuclear cells.

Conclusions Resveratrol significantly ameliorated myocardial injury and preserved cardiac function in a rat model of autoimmune myocarditis. Resveratrol may be a therapeutic modality for myocarditis. (*Circ J* 2007; **71:** 397–404)

Key Words: Aging; Heart failure; Myocarditis; Resveratrol

Patients with myocarditis present a variety of clinical manifestations, such as heart failure, arrhythmia, or circulatory collapse[1,2] Although myocarditis often follows viral infection,[3] its pathogenesis is not fully understood. There is substantial evidence suggesting that autoimmune responses to heart antigens, particularly cardiac myosin, following viral infection may contribute to the disease process.[4] An experimental model of autoimmune myocarditis (EAM) in Lewis rats produced by immunization with cardiac myosin is characterized by extremely severe myocardial lesions and multinucleated giant cells,[5,6] and it has been reported that the pathogenesis of both human giant-cell myocarditis and viral myocarditis resembles that of EAM.[7]

Resveratrol is an active ingredient of Polygonum capsidatum, a plant known for its medical use, as well as being present in peanuts and grapevines. The presence of resveratrol in red wine raises interest in this compound, because the consumption of red wine is known to reduce the risk of cardiovascular diseases.[8] The biological effects of resveratrol include protection of cells from lipid accumulation, chemoprevention, immunomodulation, antiproliferation, and differentiation.[9,10] Recent focus has been on the use of resveratrol in the treatment of cardiovascular disease because it has potent cardioprotective properties against ischemia-reperfusion injury in rat hearts,[11,12] as well as inhibiting angiotensin II-increased cardiomyocyte hypertrophy[13] and enhancing myocardial angiogenesis, both in vivo and in vitro, by induction of vascular endothelial growth factor.[14]

Silent information regulator 2 (Sir2) is a member of the sirtuin deacetylase family of enzymes that removes acetyl groups from lysine residues in histones and other proteins in a NAD-dependent manner.[15,16] SIRT1 is a mammalian ortholog of the Sir2 protein. Caloric restriction extends the life span of animals and a recent study has identified Sir2 as mediating the effects of caloric restriction.[17] Overexpression of Sir2 extends the lifespan in model organisms. SIRT1 deacetylates a variety of proteins, inducing p53, and has cytoprotective effects.[18] It has been reported that resveratrol may modulate Sir2 activity.[19]

Because resveratrol has both cardioprotective and immunomodulatory effects, it may favorably modulate the myocardial injury induced by myocarditis, which we investigated in a rat model of EAM.

Methods

Animals

Female Lewis rats (8 weeks old) were purchased from Charles River (Kanagawa, Japan). Animal care and experimental protocol were approved by the Institutional Animal Care and Use Committee of Kitasato University.

Immunization

Antigen was prepared from porcine hearts by previously described procedures.[20] The cardiac myosin was emulsified with an equal volume of complete Freund's adjuvant supplemented with Mycobacterium tuberculosis H37Ra (Difco, Detroit, MI, USA) to a final concentration of 5 mg/ml. The

(Received August 17, 2006; revised manuscript received November 28, 2006; accepted December 5, 2006)

Department of Internal Medicine and Cardiology, Kitasato University School of Medicine, Sagamihara, Japan

Mailing address: Tetsuo Shioi, MD, Department of Cardiovascular Medicine, Graduate School of Medicine, Kyoto University, 54 Kawahara-cho, Shogoin, Sakyo-ku, Kyoto 606-8507, Japan. E-mail: tshioi@kuhp.kyoto-u.ac.jp

emulsified solution (0.25 ml) or adjuvant alone was subcutaneously injected into the footpads of rats. The day of myosin injection was defined as day 0.

Experimental Protocols

Resveratrol (Sigma, St Louis, MO, USA: lot number 065K5203) was dissolved in dimethylsulfoxide (DMSO) at concentration of 20 mg/ml, and 0.5 ml of resveratrol dissolved in DMSO or the same amount of DMSO alone was injected intraperitoneally into the rats once daily. The dose of resveratrol was equivalent to 50 mg/kg.

Protocol 1 Vehicle or resveratrol was administered to rats from 1 day prior to immunization to 14 days afterward. The rats were killed after echocardiographic examination 14 days after immunization. Body weight, heart weight, and tibial length were measured. The hearts were used for analysis of histology, gene expression, and protein expression.

Protocol 2 Vehicle or resveratrol was started 1 day before immunization and continued until echocardiographic examination 21 days later, after which the rats were killed and the same measurements taken.

Protocol 3 Vehicle or resveratrol was started 1 day after immunization, continued for 14 days and then the rats were killeded after echocardiographic examination. The weights and tibial length were measured as per the other 2 protocols.

Heart Rate (HR) and Blood Pressure (BP)

Systolic BP (SBP) and HR were recorded by the tail cuff method (Softron BP-98A, Tokyo, Japan)[21] For measuring SBP, rats were placed in a warm chamber maintained at 40°C for 10 min in an individual Plexiglas restrainer. Three pressure measurements were recorded for each rat, and the average SBP was calculated.

Echocardiography

Transthoracic echocardiographic analysis was performed using a ProSound SSD-4000 (ALOKA, Tokyo, Japan) with a 7.5-MHz imaging transducer. 2-2-2 tribromoethanol (Aldrich, 0.4–0.6 mg/kg) was used for anesthesia. M-mode echocardiography was performed at the papillary muscle level, and the left ventricular end-diastolic dimension, end-systolic dimension and left ventricular posterior wall thickness were measured; fractional shortening (FS) was calculated as described[22]

Western Blotting

The hearts were removed and immediately frozen in liquid nitrogen. Lysates were obtained by homogenization of tissue in ice-cold buffer as described[22] Cardiac tissue lysates were subjected to sodium dodecyl sulfate polyacrylamide gel electrophoresis, and the proteins were transferred onto polyvinylidene difluoride membranes as described[22] For analysis of SIRT1, the blots were probed with the anti-Sir2 antibody (1:2,000 Upstate Biotechnology, Lake Placid, NY, USA) or anti-glyceraldehye-3-phosphate dehydrogene antibody (GAPDH; 1:5,000, Research Diagnosis, Flandeuns, NJ, USA).

Quantitative Reverse Transcription (RT)-Polymerase Chain Reaction (PCR)

RNA was prepared from heart tissue by the acid-guanidinium-phenol chloroform method. cDNA was synthesized using the SuperScript first-strand synthesis system (Invitrogen, Carlsbad, CA, USA) and then subjected to PCR with SYBR green (Applied Biosystems, Foster City, CA, USA) as the detected fluoroprobe. Incorporation of the SYBR green dye into the PCR products was monitored in a real-time manner with the ABI PRISM 7900HT Sequence Detection System, and the threshold cycle, which defines the PCR cycle at which exponential growth of PCR products begins, was calculated. The PCR reactions were cycled 35 times by a 3-step cycle procedure (denaturation 95°C, 15 s; annealing 60°C, 30 s; extension 72°C, 30 s). mRNA levels of B-type natriuretic peptide (BNP), tumor necrosis factor-α (TNF-α), inducible nitric oxide synthase (iNOS), manganese superoxide dismutase (Mn-SOD), copper/zinc superoxide dismutase (Cu/Zn-SOD), and SIRT1 were measured. Each of the RNA samples was normalized with an endogenous control (GAPDH mRNA). The primers used for the PCR analysis was designed using OLIGO Primer Analysis Software (TaKaRa, Kyoto, Japan) and oligonucleotides were synthesized at Invitrogen (Tokyo, Japan). The primer sequences were as follows:

BNP; sense 5'-TTCCGGATCCAGGAGAGACTT-3', antisense 5'-CCTAAAACAACCTCAGCCCGT-3', SIRT1; sense 5'-TTGGCACCGATCCTCGAA-3', antisense 5'-ACAGAAACCCCAGCTCCA-3',TNF-α; sense 5'-TGATCGGTCCCAACAAGGA-3', antisense 5'-TGCTTGGTGGTTTGCTACGA-3', iNOS; sense 5'-GAAAACCCCAGGTGCTATTCC-3', antisense 5'-CATTCTGTGCAGTCCCAGTGA-3', Mn-SOD sense 5'-ACCACGCGACCTACGTGAAC-3', antisense 5'-TGCAGGCTGAAGAGCAACCT-3', Cu/Zn-SOD sense 5'-CGAGCATGGGTTCCATGTC-3', antisense 5'-CTGGACCGCCATGTTTCTTAG-3',GAPDH sense 5'-AGGTCGGTGTGAACGGATTTG-3', antisense 5'-TGACTGTGCCGTTGAACTTGC-3'.

Histopathology

The rats were killed on day 14 and their hearts were fixed in 3.7% formaldehyde, embedded in paraffin and sectioned. The sections were stained by the hematoxylin–eosin or Mallory–Azan method and the microscopic findings were expressed as infiltration and fibrosis scores for the respective stains. Morphometric quantification was performed with Mac-Scope Image software (version 2.59; Mitani Corp, Fukui, Japan) on a Macintosh computer[23] The outline of the area of cell infiltration or fibrosis was traced by hand, the profile area was assessed automatically and the area ratio (affected area/total area in percent) was calculated.

Immunohistochemical Analysis of SIRT1 Expression

Heart tissue was embedded in OCT compound, snapfrozen on dry ice, and stored at –70°C. Samples were sectioned on a cryostat at 10 μm and then fixed for 5 min in acetone at 4°C. The sections were incubated with anti-SIRT1 antibody (rabbit IgG, Santa Cruz Biotechnology, Santa Cruz, CA, USA) and anti-actinin antibody (mouse IgG, Sigma) at 4°C overnight. Next, sections were incubated with fluorescent isothiocyanate-labeled anti-rabbit IgG and rhodamine-labeled anti-mouse IgG antibodies at room temperature for 30 min. Nuclei were stained using TOTO-3 (Invitorogen Carlsbad, CA, USA). Sections were analyzed by confocal microscopy (Carl Zeiss, Oberkochen, Germany).

Statistical Analysis

All values are expressed as mean ± SEM. Differences between groups were compared using Student's t-tests. A p-value <0.05 was considered as significant.

Table 1 Blood Pressure and HR of EAM Rats Treated With Resveratrol for 2 Weeks

	Unimmunized		*Myosin-immunized*	
	Vehicle	*Resveratrol*	*Vehicle*	*Resveratrol*
No. animals	5	5	8	8
SBP (mmHg)	115.2±3.9	118.5±6.6	96.4±5.1*	108.8±6.4
HR (beats/min)	323.7±10.7	353.9±16.2	372.3±14.1*	397.2±14.7

Resveratrol was started 1 day before immunization, and given daily for 2 weeks. Results are mean±SEM.
**p<0.05 vs unimmunized rats treated with vehicle or resveratrol.*
HR, heart rate; EAM, experimental model of autoimmune myocarditis; SBP, systolic blood pressure.

Table 2 Echocardiographic Data of EAM Rats Treated With Resveratrol for 2 Weeks

	Unimmunized		*Myosin-immunized*	
	Vehicle	*Resveratrol*	*Vehicle*	*Resveratrol*
No. animals	5	5	8	6
HR (beats/min)	444±13	429±6	405±9*	385±10*
Diastolic posterior wall thickness (mm)	1.54±0.12	1.62±0.16	1.85±0.13	1.64±0.08
LV diastolic diameter (mm)	4.70±0.11	4.78±0.17	4.56±0.15	4.51±0.24
LV systolic diameter (mm)	1.46±0.11	1.36±0.11	2.51±0.17*	1.91±0.22†
FS (%)	68.5±3.0	71.6±1.7	44.6±3.4*	58.2±3.0*†

Resveratrol was started 1 day before immunization, and given daily for 2 weeks.
LV, left ventricle; FS, fractional shortening. Other abbreviations see in Table 1.
Results are mean±SEM.
**p<0.05 vs unimmunized rats treated with vehicle or resveratrol, †p<0.05 vs vehicle-treated myosin-immunized rats.*

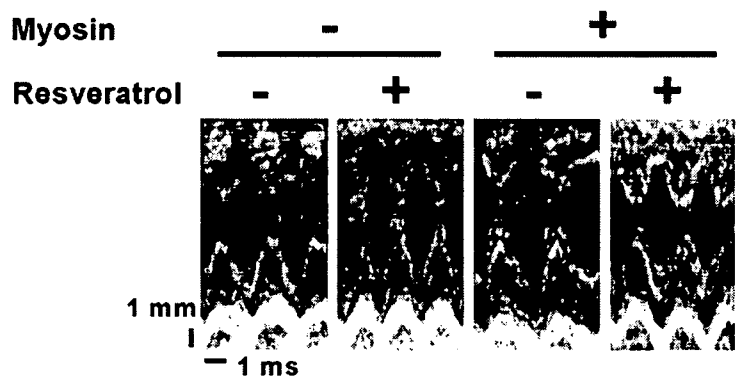

Fig 1. Echocardiographic analysis of experimental model of autoimmune myocarditis rats treated with resveratrol. (Left to right) Vehicle-treated unimmunized rat, resveratrol-treated unimmunized rat, vehicle-treated myosin-immunized rat, resveratrol-treated myosin-immunized rat. Fractional shortening of vehicle-treated myosin-immunized rats was decreased compared with vehicle-treated unimmunized rats. Resveratrol treatment attenuated the decrease of fractional shortening in the myosin-immunized rats.

Table 3 Postmortem Analysis of EAM Rats Treated With Resveratrol for 2 Weeks

	Unimmunized		*Myosin-immunized*	
	Vehicle	*Resveratrol*	*Vehicle*	*Resveratrol*
No. animals	5	5	8	8
Body weight (g)	177.2±2.0	182.2±4.3	171.0±3.1	184.4±2.3†
Heart weight (mg)	590.4±6.1	589.6±16.0	1,023.6±86.4*	739.4±60.9†
Lung weight (mg)	1,045.2±31.1	1,004.6±55.9	1,039.3±26.7	1,013.0±14.3
Tibial length (mm)	33.6±0.2	33.2±0.1	32.1±0.2*	32.3±0.2*
Heart weight/body weight (mg/g)	3.34±0.07	3.23±0.04	6.05±0.58*	4.04±0.99†
Lung weight/body weight (mg/g)	5.90±0.18	5.51±0.25	6.08±0.14	5.50±0.07
Heart weight/tibial length (mg/mm)	17.6±0.2	17.8±0.4	31.9±2.6*	22.9±1.9*†
Lung weight/tibial length (mg/mm)	31.1±0.8	30.3±1.8	32.4±0.7	31.4±0.4

Resveratrol was started 1 day before immunization, and given daily for 2 weeks.
Abbreviation see in Table 1. Results are mean±SEM.
**p<0.05 vs unimmunized rats treated with vehicle or resveratrol, †p<0.05 vs vehicle-treated myosin-immunized rats.*

Results

HR and BP

At 14 days after immunization, we examined the effect of resveratrol on HR and BP. The SBP of vehicle-treated myosin-immunized rats was decreased compared with that of vehicle-treated unimmunized rats (96.4±5.1 mmHg vs 115.2±3.9 mmHg, p<0.05, Table 1). The BP of resveratrol-treated myosin-immunized rats was not different from that of vehicle-treated unimmunized rats.

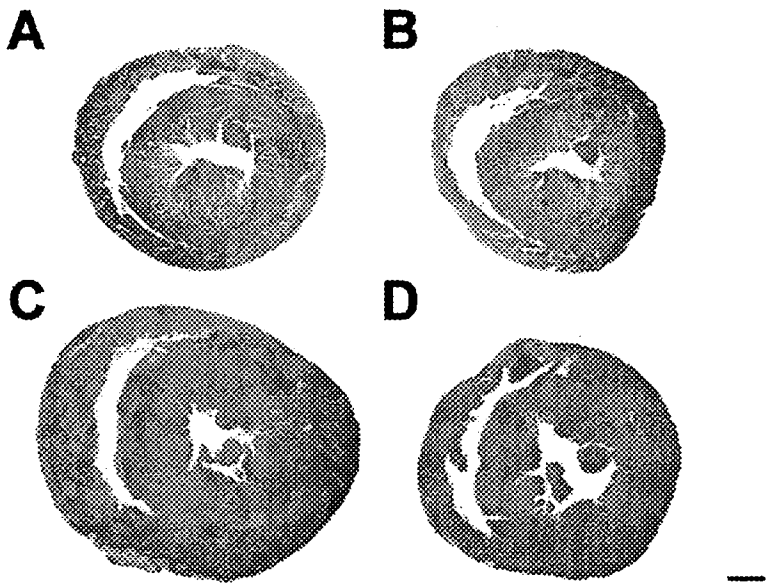

Fig 2. Macroscopic analysis of experimental model of autoimmune myocarditis rats treated with resveratrol. (A) Vehicle-treated unimmunized rat, (B) resveratrol-treated unimmunized rat, (C) vehicle-treated myosin-immunized rat, and (D) resveratrol-treated myosin-immunized rat. The left ventricle was dilated and wall thickness was increased in vehicle-treated myosin-immunized rats. Resveratrol attenuated cardiac enlargement. Bar = 1 mm.

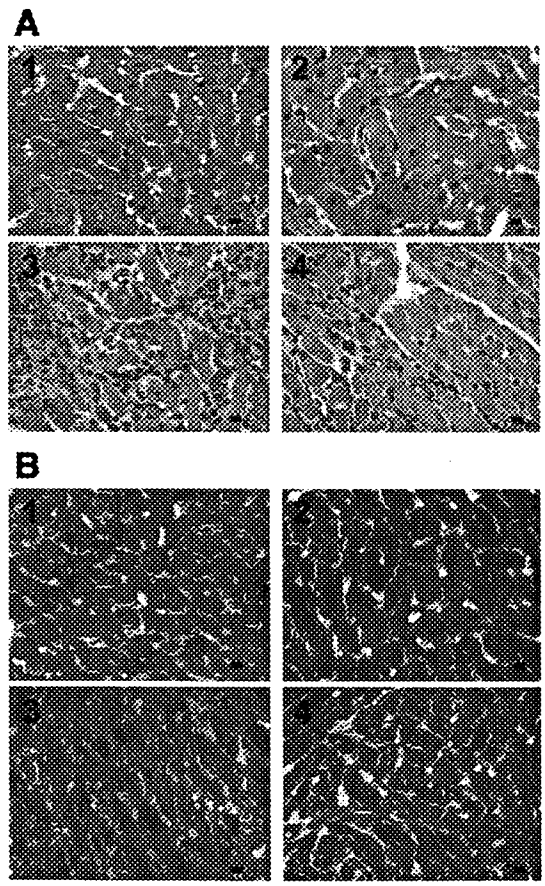

Fig 3. Effect of resveratrol on (A) cellular infiltration and (B) fibrosis. (A) Representative images of (1) vehicle-treated unimmunized rats, (2) resveratrol-treated unimmunized rats, (3) vehicle-treated myosin-immunized rats, and (4) resveratrol-treated myosin-immunized rats. Resveratrol attenuated cellular infiltration. Bars = 10 μm. (B) Representative images of (1) vehicle-treated unimmunized rats, (2) resveratrol-treated unimmunized rats, (3) vehicle-treated myosin-immunized rats, and (4) resveratrol-treated myosin-immunized rats, are shown. Resveratrol attenuated fibrosis. Bars = 10 μm.

Echocardiographic Analysis

At 14 days after immunization, we examined the effect of resveratrol on cardiac function using echocardiography (Table 2, Fig 1). The FS of vehicle-treated myosin-immunized rats was decreased compared with that of vehicle-treated unimmunized rats (44.6±3.4% vs 68.5±3.0%, $p < 0.05$). Resveratrol treatment attenuated the decrease in FS in myosin-immunized rats, thus preserving the cardiac function of EAM rats.

Postmortem Analysis

At 14 days after immunization, the heart weight/tibial length ratio of myosin-immunized rats was increased by 1.81-fold compared with vehicle-treated unimmunized rats (31.9±2.6 mg/mm vs 17.6±0.2 mg/mm, $p < 0.05$, Table 3, Fig 2). In contrast, the heart weight/tibial length ratio of resveratrol-treated myosin-immunized rats was increased by 1.29-fold compared with resveratrol-treated unimmunized rats (22.9±1.9 mg/mm vs 17.8±0.4 mg/mm, $p < 0.05$). Thus, resveratrol significantly suppressed the increase in heart weight of EAM rats.

Histopathological Analysis

The area of cell infiltration in resveratrol-treated myosin-immunized rats was significantly decreased compared with vehicle-treated myosin-immunized rats (2.6±1.5% vs 26.4±3.6%, $p < 0.05$; Fig 3, Table 4). The area of fibrosis in resveratrol-treated myosin-immunized rats was decreased from that of vehicle-treated myosin-immunized rats (5.5±3.2% vs 28.0±4.6%, $p < 0.05$; Fig 3, Table 4). Overall, resveratrol attenuated the inflammation and fibrosis of the myocardium of EAM rats.

BNP Gene Expression

BNP mRNA of myosin-immunized rats was increased by 12.4±2.2-fold compared with vehicle-treated unimmunized rats (Table 5). BNP mRNA of resveratrol-treated myosin-immunized rats was increased by 1.6±0.5-fold compared with vehicle-treated unimmunized rats. Resveratrol significantly suppressed the increase in BNP mRNA in the myocardium of EAM rats.

Table 4 Cellular Infiltration and Fibrosis of the Myocardium of EAM Rats Treated With Resveratrol for 2 Weeks

	Myosin-immunized	
	Vehicle	*Resveratrol*
No. animals	6	6
Cellular infiltration area ratio (%)	26.4±3.6	2.6±1.5*
No. animals	6	6
Fibrosis area ratio (%)	28.0±4.6	5.5±3.2*

Resveratrol was started 1 day before immunization, and given daily for 2 weeks.
Abbreviation see in Table 1. Results are mean±SEM.
**p<0.05 vs vehicle-treated myosin-immunized rats.*

Table 5 BNP mRNA in the Myocardium of EAM Rats Treated With Resveratrol for 2 Weeks

	Unimmunized		*Myosin-immunized*	
	Vehicle	*Resveratrol*	*Vehicle*	*Resveratrol*
No. animals	4	4	5	5
BNP mRNA (units)	1.00±0.25	0.41±0.13	12.42±2.22*	1.61±0.46†

Resveratrol was started 1 day before immunization, and given daily for 2 weeks.
The mean value of vehicle-treated unimmunized rats was defined as one unit.
BNP, B-type natriuretic peptide. Other abbreviation see in Table 1. Results are mean±SEM.
**p<0.05 vs unimmunized rats treated with vehicle or resveratrol, †p<0.05 vs vehicle-treated myosin-immunized rats.*

Table 6 TNF-α and iNOS mRNA in the Myocardium of EAM Rats Treated With Resveratrol for 2 Weeks

	Unimmunized		*Myosin-immunized*	
	Vehicle	*Resveratrol*	*Vehicle*	*Resveratrol*
No. animals	5	5	5	5
TNF-α mRNA (units)	1.00±0.16	1.30±0.16	46.18±14.4*	1.54±0.25†
iNOS mRNA (units)	Undetectable	Undetectable	283.82±115.81*	1.00±0.40*,†

Resveratrol was started 1 day before immunization, and given daily for 2 weeks.
The mean value of vehicle-treated unimmunized rats was defined as 1 unit for TNF-α mRNA.
The mean value of resveratrol-treated immunized rats was defined as 1 unit for iNOS mRNA.
TNF-α, tumor necrosis factor-α; iNOS, inducible nitric oxide synthase. Other abbreviation see in Table 1.
Results are mean±SEM.
**p<0.05 vs unimmunized rats treated with vehicle or resveratrol, †p<0.05 vs vehicle-treated myosin-immunized rats.*

Table 7 Mn-SOD and Cu/Zn-SOD mRNA in the Myocardium of EAM Rats Treated With Resveratrol for 2 Weeks

	Unimmunized		*Myosin-immunized*	
	Vehicle	*Resveratrol*	*Vehicle*	*Resveratrol*
No. animals	5	5	5	5
Mn-SOD mRNA (units)	1.00±0.24	0.94±0.33	7.51±1.39*	1.42±0.35†
Cu/Zn-SOD mRNA (units)	1.00±0.07	1.10±0.36	3.03±1.11*	1.47±0.43†

Resveratrol was started 1 day before immunization, and was given daily for 2 weeks.
The mean value of vehicle-treated unimmunized rats was defined as 1 unit.
Mn-SOD, manganese superoxide dismutase; Cu/Zn-SOD, copper/zinc superoxide dismutase. Other abbreviation see in Table 1.
Results are mean±SEM.
**p<0.05 vs unimmunized rats treated with vehicle or resveratrol, †p<0.05 vs vehicle-treated myosin-immunized rats.*

Expression of Inflammatory Markers

The levels of both TNF-α and iNOS mRNA were analyzed using quantitative RT-PCR (Table 6). TNF-α mRNA was increased by 46.2±14.4-fold, and resveratrol suppressed TNF-α expression. iNOS mRNA was increased in EAM rats and resveratrol significantly decreased its expression.

Expression of Antioxidant Genes

The level of expression of the antioxidant enzymes, Mn-SOD and Cu/Zn-SOD, was analyzed using quantitative RT-PCR (Table 7). Mn-SOD mRNA increased by 7.5±1.4-fold, and Cu/Zn-SOD mRNA by 3.0±1.1-fold in the myocardium of EAM rats. Resveratrol significantly attenuated the expression of both enzymes.

SIRT1 Expression

The level of SIRT 1 mRNA was analyzed using quantitative RT-PCR. SIRT1 mRNA was increased by 2.2±0.2-fold in vehicle-treated myosin-immunized rats compared with vehicle-treated unimmunized rats (Fig 4A). The amount of SIRT1 protein was also increased in vehicle-treated myosin-immunized rats (Fig 4B). The immunofluorescence study showed that the SIRT1 protein was mainly localized in infiltrating mononuclear cells (Fig 5).

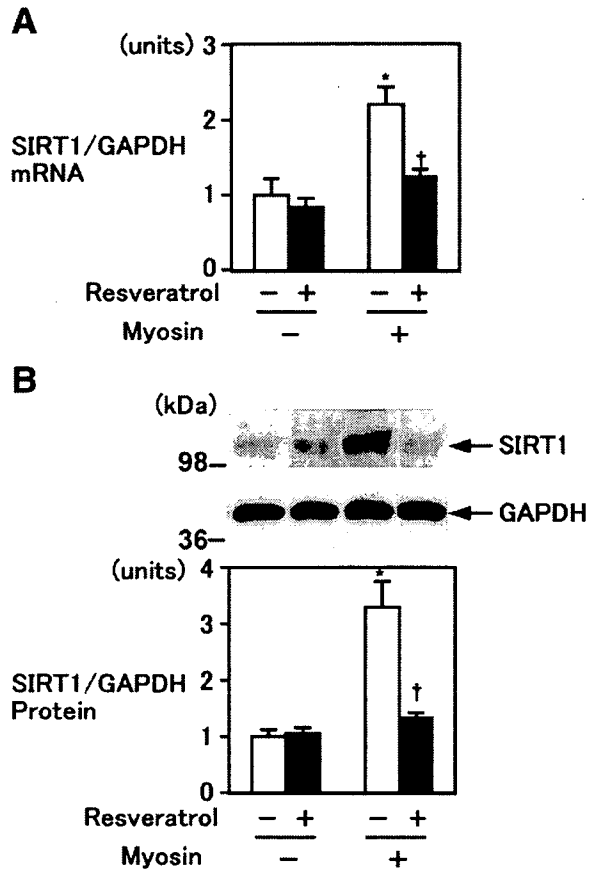

Fig4. Expression of SIRT1, a mammalian ortholog of silent information regulator 2 protein in the heart of experimental model of autoimmune myocarditis. (A) SIRT1 mRNA expression measured by quantitative reverse transcription-polymerase chain reaction was increased in the hearts of myosin-immunized rats. (B) SIRT1 protein expression. Representative Western blot of SIRT1 (Upper panel), and the result of quantitative densitometric analysis (Lower panel). SIRT1 protein was increased in the hearts of myosin-immunized rats. Vehicle-treated unimmunized rats (n=4), resveratrol-treated unimmunized rats (n=4), vehicle-treated myosin-immunized rats (n=5), and resveratrol-treated myosin-immunized rats (n=5) were used for the analysis. *p<0.05 vs unimmunized rats treated with vehicle, †p<0.05 vs vehicle-treated myosin-immunized rats. The mean value of vehicle-treated unimmunized rat was defined as 1 unit. GAPDH, glyceraldehye-3-phosphate dehydrogene.

Effect of Resveratrol at 3 Weeks After Immunization

Three weeks after immunization (ie, Protocol 2), the FS of resveratrol-treated rats was greater than that of vehicle-treated rats (66.7±3.0% vs 34.4±4.4%, p<0.05, Table 8). The heart weight/tibial length ratio of the resveratrol-treated rats was smaller compared with vehicle-treated rats (25.4±3.5 mg/mm vs 36.0±2.3 mg/mm, p<0.05, Table 9). Thus, resveratrol effectively prevented myocarditis at 3 weeks after the immunization.

Effect of Resveratrol on EAM After Immunization

When vehicle or resveratrol was started 1 day after immunization (ie, Protocol 3), the FS of resveratrol-treated rats was greater than that of the vehicle-treated rats (63.8±3.0% vs 36.3±4.3%, p<0.05, Table 10). The heart weight/tibial length ratio of resveratrol-treated rats was smaller compared with vehicle-treated rats (19.9±2.0 mg/mm vs 30.4±2.4 mg/mm, p<0.05, Table 11). Thus, resveratrol also attenuated myocarditis when it was given after immunization.

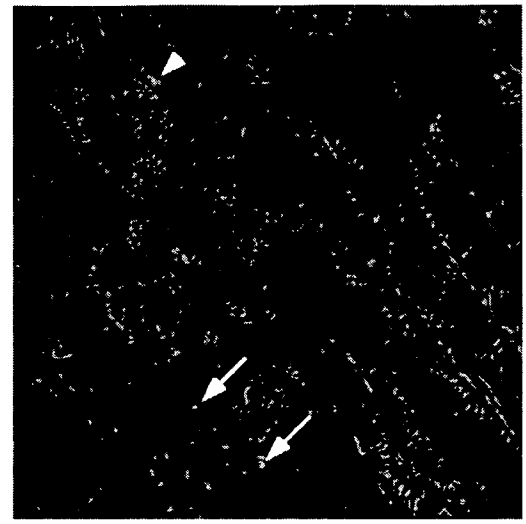

Fig5. Localization of SIRT1 in the myocardium of experimental model of autoimmune myocarditis was examined by immunofluorescence analysis. The SIRT1 protein was mainly localized in infiltrating mononuclear cells (arrow). Some of the cardiac myocytes close to infiltrating mononuclear cells were also positive for SIRT1 immunoreactivity (arrowhead). Green, SIRT1; red, actinin; blue, nuclei.

Table 8 Echocardiographic Data of EAM Rats Treated With Resveratrol for 3 Weeks After Immunization

	Vehicle	*Resveratrol*
No. animals	*10*	*8*
HR (beats/min)	*366±14*	*400±7*
Diastolic posterior wall thickness (mm)	*2.63±0.21*	*1.71±0.11**
LV diastolic diameter (mm)	*5.19±0.36*	*4.68±0.14*
LV systolic diameter (mm)	*3.49±0.41*	*1.58±0.19**
FS (%)	*34.4±4.4*	*66.7±3.0**

Resveratrol was started 1 day before immunization, and given daily for 21 days after immunization.
Abbreviations see in Tables 1,2. Results are mean±SEM.
**p<0.05 vs vehicle-treated myosin-immunized rats.*

Table 9 Postmortem Analysis of EAM Rats Treated With Resveratrol for 3 Weeks After Immunization

	Vehicle	*Resveratrol*
No. animals	*10*	*10*
Body weight (g)	*170.0±2.1*	*181.9±5.2**
Heart weight (mg)	*1,224.3±77.5*	*853.1±118.0**
Lung weight (mg)	*1,291.8±122.8*	*1,194.6±110.7*
Tibial length (mm)	*34.1±0.2*	*33.6±0.2**
Heart weight/body weight (mg/g)	*7.24±0.51*	*4.80±0.74**
Lung weight/body weight (mg/g)	*7.59±0.71*	*6.70±0.78*
Heart weight/tibial length (mg/mm)	*36.0±2.3*	*25.4±3.5**
Lung weight/tibial length (mg/mm)	*38.0±3.7*	*35.6±3.3*

Resveratrol was started 1 day before immunization, and given daily for 21 days after immunization.
Abbreviation see in Table 1. Results are mean±SEM.
**p<0.05 vs vehicle-treated myosin-immunized rats.*

Discussion

In this study, resveratrol preserved the cardiac function

Table 10 Echocardiographic Data of EAM Rats Treated With Resveratrol Starting 1 Day After Immunization

	Vehicle	*Resveratrol*
No. animals	7	9
HR (beats/min)	380±17	402±10
Diastolic posterior wall thickness (mm)	2.17±0.11	1.58±0.49*
LV diastolic diameter (mm)	4.89±0.24	4.67±0.17
LV systolic diameter (mm)	3.10±0.21	1.73±0.18*
FS (%)	36.3±4.3	63.8±3.0*

Resveratrol was started 1 day after immunization and given daily for 2 weeks.
Abbreviations see in Tables 1,2. Results are mean±SEM.
**p<0.05 vs vehicle-treated myosin-immunized rats.*

Table 11 Postmortem Analysis of EAM Rats Treated With Resveratrol Starting 1 Day After Immunization

	Vehicle	*Resveratrol*
No. animals	9	9
Body weight (g)	166.8±1.9	167.1±2.8
Heart weight (mg)	1,012.7±77.2	668.3±68.2*
Lung weight (mg)	1,117.3±29.6	988.0±31.2*
Tibial length (mm)	33.4±0.2	33.6±0.2
Heart weight/body weight (mg/g)	6.06±0.45	4.02±0.43*
Lung weight/body weight (mg/g)	6.71±0.23	5.90±0.14*
Heart weight/tibial length (mg/mm)	30.4±2.4	19.9±2.0*
Lung weight/tibial length (mg/mm)	33.5±0.9	29.4±0.9*

Resveratrol was started 1 day after immunization, and given daily for 2 weeks.
Abbreviation see in Table 1. Results are mean±SEM.
**p<0.05 vs vehicle-treated myosin-immunized rats.*

of EAM rats. It attenuated the increase in heart weight and suppressed the expression of pro-inflammatory genes. The attenuation of myocardial injury was associated with a decrease in antioxidant gene expressions. SIRT1, a possible effector of resveratrol, was increased in the myocardium of EAM rats, and was mainly localized in infiltrating mononuclear cells.

In this study, we used DMSO as the solvent, because we needed to administer a relatively high dose of resveratrol, and it is known to have an immunomodulatory function[24,25] We administered 0.5 ml of DMSO or the same amount of saline to myosin-immunized rats for 14 days. The heart weight/tibial length ratio of DMSO-treated myosin-immunized rats was reduced compared with saline-treated myosin-immunized rats (31.9±2.6 mg/mm vs 41.8±1.6 mg/mm, $p<0.05$), although the effect of DMSO was much weaker than resveratrol dissolved in DMSO. Thus, it is possible that the strong suppression of the inflammatory response was a synergistic effect of DMSO and resveratrol.

The HR of myosin-immunized rats was higher than that of unimmunized rats on BP measurement without anesthesia, whereas that of myosin-immunized rats was lower than in unimmunized rats on echocardiographic analysis with anesthesia. It is likely that the response of myosin-immunized rats to anesthesia was different from that of unimmunized rats.

The mechanism of resveratrol's attenuation of EAM is unknown. Resveratrol is reported to reduce oxidative stress[26,27] and in this study, the expression of oxidative stress-related genes (Mn-SOD, Cu/Zn-SOD) were increased in the heart of myosin-immunized rats. This increase of both was likely the result of increased oxidative stress, and attenuation of myocarditis was associated with a decrease of Mn-SOD and Cu/Zn-SOD. Thus, resveratrol may ameliorate EAM by reducing oxidative stress because oxygen radical scavengers are known to attenuate myocarditis[28,29]

Alternatively, resveratrol may modulate EAM by acting on SIRT1, which was increased in the myocardium of myosin-immunized rats, and mainly localized in the infiltrating mononuclear cells. Fibroblasts deficient in SIRT1 proliferate more rapidly than wild-type cells.[30] SIRT1 induces cell-cycle arrest by activating the Forkhead transcription factor.[31] Resveratrol also inhibits the proliferation of some tumors?[9,10] Thus, it is possible that resveratrol modulates the activity of SIRT1 in immune cells, and limits lymphocyte proliferation. However, the role of SIRT1 in immune cells is currently unknown and further studies are needed to clarify its role in EAM.

We used a relatively high dose of resveratrol. The HW/TL ratio of myosin-immunized rats treated with a lower dose of resveratrol (10 mg/kg per day) was not different from that of vehicle-treated myosin-immunized rats (43.9±6.7 mg/mm vs 43.3±3.9 mg/mm). Resveratrol is reported to have different effects on immune cells, depending on the dose and experimental condition.[32,33]

In conclusion, resveratrol effectively ameliorated EAM. Although further study is needed, resveratrol may be a therapeutic modality for myocarditis.

Acknowledgments

This study was supported in part by grants from the Japan Society for the Promotion of Science (15390252), the Japan Heart Foundation, the Japan Foundation of Cardiovascular Research, the NOVARTIS Foundation for the Promotion of Science, the Mochida Memorial Foundation for Medical and Pharmaceutical Research, the Takeda Medical Research Foundation, the Kanagawa Nanbyo Foundation, the Takeda Science Foundation (to T.S.), and the Japan Society for the Promotion of Science (16590713), Postgraduate Research Project of Kitasato University (to T.I.).

References

1. Drory Y, Turetz Y, Hiss Y, Lev B, Fisman EZ, Pines A, et al. Sudden unexpected death in persons less than 40 years of age. *Am J Cardiol* 1991; **68:** 1388–1392.
2. Hiramitsu S, Morimoto S, Kato S, Uemura A, Ohtsuki M, Kato Y, et al. Clinical course of myocarditis through the acute, fulminant and fatal chronic stages: An autopsy case. *Circ J* 2006; **70:** 1086–1090.
3. Woodruff JF. Viral myocarditis: A review. *Am J Pathol* 1980; **101:** 425–484.
4. Lauer B, Padberg K, Schultheiss HP, Strauer BE. Autoantibodies against human ventricular myosin in sera of patients with acute and chronic myocarditis. *J Am Coll Cardiol* 1994; **23:** 146–153.
5. Kodama M, Matsumoto Y, Fujiwara M, Masani F, Izumi T, Shibata A. A novel experimental model of giant cell myocarditis induced in rats by immunization with cardiac myosin fraction. *Clin Immunol Immunopathol* 1990; **57:** 250–262.
6. Kawada H, Niwano S, Niwano H, Yumoto Y, Wakisaka Y, Yuge M, et al. Tumor necrosis factor-α-downregulates the voltage gated outward K+ current in cultured neonatal rat cardiomyocytes: A possible cause of electrical remodeling in diseased hearts. *Circ J* 2006; **70:** 605–609.
7. Ishiyama S, Hiroe M, Nishikawa T, Abe S, Shimojo T, Ito H, et al. Nitric oxide contributes to the progression of myocardial damage in experimental autoimmune myocarditis in rats. *Circulation* 1997; **95:** 489–496.
8. Sato M, Maulik N, Das DK. Cardioprotection with alcohol: Role of both alcohol and polyphenolic antioxidants. *Ann NY Acad Sci* 2002; **957:** 122–135.
9. Shazib P. Resveratrol: From grapevines to mammalian biology. *FASEB J* 2003; **17:** 1975–1985.
10. Lucie F. Biological effects of resveratrol. *Life Sci* 2000; **66:** 663–673.
11. Dernek S, Ikizler M, Erkasap N, Ergun B, Koken T, Yilmaz K, et al. Cardioprotection with resveratrol pretreatment: Improved beneficial

effects over standard treatment in rat hearts after global ischemia. *Scand Cardiovasc J* 2004; **38:** 245–254.
12. Ray PS, Maulik G, Cordis GA, Bertelli AA, Bertelli A, Das DK. The red wine antioxidant resveratrol protects isolated rat hearts from ischemia reperfusion injury. *Free Radic Biol Med* 1999; **27:** 160–169.
13. Cheng TH, Liu JC, Lin H, Shih NL, Chen YL, Huang MT, et al. Inhibitory effect of resveratrol on angiotensin II-induced cardiomyocyte hypertrophy. *Naunyn Schmiedebergs Arch Pharmcol* 2004; **369:** 239–244.
14. Shigeaki K, Lijun Z, Masahiko M, Nilanjana M. Resveratrol enhances neovascularization in the infarcted rat myocardium through the induction of thioredoxin-1, heme oxigenase-1 and vascular endothelial growth factor. *J Mol Cell Cardiol* 2005; **39:** 813–822.
15. Blander G, Guarente L. The Sir2 family of protein deacetylases. *Annu Rev Biochem* 2004; **73:** 417–435.
16. Hiroaki D, Mitsutoki H, Hitomi M, Satoko A, Takayuki O, Makoto M, et al. Silent information regulator 2 potentiates Foxo1-mediated transcription through its deacetylase actyvity. *Proc Natl Acad Sci USA* 2004; **101:** 10042–10047.
17. Leonard G, Frederic P. Calorie Restriction-the Sir2 connection. *Cell* 2005; **120:** 473–482.
18. Araki T, Sasaki Y, Milbrandt J. Increased nuclear NAD biosynthesis and SIRT1 activation prevent axonal degeneration. *Science* 2004; **305:** 1010–1013.
19. Howitz KT, Bitterman KJ, Cohen HY, Lamming DW, Lavu S, Wood JG, et al. Small molecule activators of sirtuins extend Saccharomyces cerevisiae lifespan. *Nature* 2003; **425:** 191–196.
20. Inomata T, Hanawa H, Miyanishi T, Yajima E, Nakayama S, Maita T, et al. Localization of porcine cardiac myosin epitopes that induce experimental autoimmune myocarditis. *Circ Res* 1995; **76:** 726–733.
21. Bunag RD. Validation in awake rats of a tail-cuff method for measuring systolic pressure. *J Appl Physiol* 1973; **34:** 279–282.
22. Shioi T, Kang PM, Douglas PS, Hampe J, Yballe CM, Lawitts J, et al. The conserved phosphoinositide 3-kinase pathway determines heart size in mice. *EMBO J* 2000; **19:** 2537–2548.
23. Kameda Y. Mash1 is required for glomus cell formation in the mouse carotid body. *Dev Biol* 2005; **283:** 128–139.
24. Milner L, de Chadarevian J, Goodyer P, Mills M, Kaplan B. Amelioration of murine lupus nephritis by dimethylsulfoxide. *Clin Immunol Immunopathol* 1987; **45:** 259–267.
25. Pestronk A, Teoh R, Sims C, Drachman DB. Effects of dimethylsulfoxide on humoral immune responses to acetylcholine receptors in the rat. *Clin Immunol Immunopathol* 1985; **37:** 172–178.
26. Shigematsu S, Ishida S, Hara M, Takahashi N, Yoshimatsu H, Sakata T, et al. Resveratrol, a red wine constituent polyphenol, prevents superoxide-dependent inflammatory responses induced by ischemia/reperfusion, platelet-activating factor, or oxidants. *Free Radic Biol Med* 2003; **34:** 810–817.
27. Sengottuvelan M, Viswanathan P, Nalini N. Chemopreventive effect of trans-resveratrol: A phytoalexin against colonic aberrant crypt foci and cell proliferation in 1,2-dimethylhydrazine induced colon carcinogenesis. *Carcinogenesis* 2006; **27:** 1038–1046.
28. Suzuki H, Matsumori A, Matoba Y, Kyu BS, Tanaka A, Fujita J, et al. Enhanced expression of superoxide dismutase messenger RNA in viral myocarditis: An SH-dependent reduction of its expression and myocardial injury. *J Clin Invest* 1993; **91:** 2727–2733.
29. Hiraoka Y, Kishimoto C, Kurokawa M, Ochiai H, Sasayama S. Effects of polyethylene glycol conjugated superoxide dismutase on coxsackievirus B3 myocarditis in mice. *Cardiovasc Res* 1992; **26:** 956–961.
30. Chua KF, Mostoslavsky R, Lombard DB, Pang WW, Saito S, Franco S, et al. Mammalian SIRT1 limits replicative life span in response to chronic genotoxic stress. *Cell Metab* 2005; **2:** 67–76.
31. Brunet A, Sweeney LB, Sturgill JF, Chua KF, Greer PL, Lin Y, et al. Stress-dependent regulation of FOXO transcription factors by the SIRT1 deacetylase. *Science* 2004; **303:** 2011–2015.
32. Gao X, Deeb D, Media J, Divine G, Jiang H, Chapman RA, et al. Immunomodulatory activity of resveratrol: Discrepant in vitro and in vivo immunological effects. *Biochem Pharmacol* 2003; **66:** 2427–2435.
33. Feng Y, Zhou W, Wu Q, Li X, Zhao W, Zou J. Low dose of resveratrol enhanced immune response of mice. *Acta Pharmacol Sin* 2002; **23:** 893–897.

ELSEVIER

International Journal of Cardiology 112 (2006) 15–20

International Journal of Cardiology

www.elsevier.com/locate/ijcard

Antigen-specific effects of autoantibodies against sarcolemmal Na–K-ATPase pump in immunized cardiomyopathic rabbits

Akiyasu Baba [a,*], Tsutomu Yoshikawa [b], Michikado Iwata [b], Toshihisa Anzai [b], Iwao Nakamura [b], Yumiko Wainai [b], Satoshi Ogawa [b], Michael Fu [c]

[a] *Department of Medicine, Kitasato Institute Hospital, 5-9-1 Shirokane Minato-ku, Tokyo, 108 8642, Japan*
[b] *Department of Medicine, Keio University School of Medicine, Tokyo, Japan*
[c] *Heart Failure Centre Medicine, Department of Medicine, Sahlgrenska University Hospital/Sahlgrenska c/o Wallenberg Laboratory, University of Gothenburg, Gothenburg, Sweden*

Received 14 April 2006; accepted 10 May 2006
Available online 24 July 2006

Abstract

Objectives: We examine antigen-specific actions of autoantibodies directed against sarcolemmal Na–K-ATPase.
Background: Autoantibodies against some receptors or pumps were detected in patients with dilated cardiomyopathy. Although immunoglobulin adsorption therapy improved cardiac function in such patients, direct pathogenic effects of autoantibodies remain to be proven.
Methods: Japanese white rabbits were immunized once a month with purified Na–K-ATPase (NKA rabbits, $n=10$) or a synthetic peptide corresponding to the second extracellular loop of beta1-adrenergic receptors (beta rabbits, $n=10$), respectively. Control rabbits ($n=10$) received vehicle in the same manner.
Results: At 6 months, cardiac hypertrophy along with increased left ventricular end-diastolic pressure was observed in both NKA and beta rabbits, and inhibitory G protein level increased in both NKA and beta rabbits. Histological findings showed similar myocyte hypertrophy and interstitial fibrosis in both rabbits. Enzymatic activities of Na–K-ATPase were lower in NKA rabbits than in other groups. Immunoblotting showed that alpha3-isoform of Na–K-ATPase was selectively reduced in myocardium from NKA rabbits.
Conclusions: Our present findings suggested that isoform-specific alterations of myocardial Na–K-ATPase activity were induced by immunizing rabbits. This was not secondary change due to cardiac hypertrophy. Thus, autoantibodies against sarcolemmal Na–K-ATPase have antigen-specific effect on the heart in vivo.

Keywords: Dilated cardiomyopathy; Autoantibodies; Na–K-ATPase

1. Introduction

Autoimmune mechanism is one of the causes of dilated cardiomyopathy (DCM) as well as genetic predisposition and viral infection. Production of anti-myocardial autoantibodies (Abs) is one of the outstanding autoimmune abnormalities in addition to persistent inflammation with alterations in cellular immunity and complement activation. Therefore, immunoadsorption (IA) therapy to remove various Abs was suggested as a new strategy to treat patients with congestive heart failure due to DCM [1]. Unsatisfactory hemodynamic improvement by IA therapy using protein-A column indicated the pathophysiological meaning of immunoglobulin G3, although the mechanism was not fully evaluated. In biopsy sample of the DCM patients, C5b-9 complex and the expression of TNF-alpha were observed along with the immunoglobulin deposits on the myocardial cell membrane [2]. This finding may provide a common mechanism leading to cardiac hypertrophy by any anti-myocardial Abs. However, we reported different clinical

* Corresponding author. Tel.: +81 3 3444 6161x4610; fax: +81 3 3448 0553.
E-mail address: baba-a@kitasato.or.jp (A. Baba).

0167-5273/$ - see front matter © 2006 Elsevier Ireland Ltd. All rights reserved.
doi:10.1016/j.ijcard.2006.05.026

backgrounds of each Abs in patients with DCM [3]. So, we postulated antigen-specific effects of Abs and performed an experiment using immunizing rabbit model.

2. Materials and methods

2.1. Immunization

Experiments were performed in 30 male Japanese white rabbits, which were 10 weeks old (1.8 to 2.2 kg). The experimental protocol was approved by our Institutional Review Board. As antigens, porcine cerebral cortex Na–K-ATPase were obtained from Sigma Chemical Co. (St. Louis, Missouri) and a synthetic peptide corresponding to the second extracellular loop of rabbit beta1-adrenergic receptors (residues 197 to 222, HWWRAESDEARR-CYNDPKCCDFVTNR) was produced by Peptide Institute, Inc. (Osaka, Japan). Twenty rabbits were randomly divided into two groups and were immunized by subcutaneous injection of each antigens (1 mg) dissolved in 1 ml of saline conjugated with 0.5 ml of complete and incomplete Freund's adjuvant (NKA rabbits: $n=10$, beta rabbits: $n=10$). Ten control rabbits received saline containing adjuvant in the same manner. All rabbits were immunized once a month over 6 months.

2.2. Enzyme-linked immunoabsorbent assay (ELISA)

Each antigen (50 μl, 50 μg/ml in 0.1 mol/l Na_2CO_3) was used to coat individual wells of a 96-well microtiter plate. The wells were then saturated with phosphate buffer saline (PBS) supplemented with 3% skim milk, 0.1% Tween-20 and 0.01% merthiolate. Sera (50 μl) diluted 1:200 were added to the coated plates and incubated overnight at 4 °C. After three washes with PBS, an affinity-purified biotinylated goat anti-rabbit IgG antibody solution, diluted 1:1000 in merthiolate, was allowed to react for 1 h at room temperature. After three washes, the bound biotinylated antibodies were detected using streptavidin-peroxidase (1 μl/ml), H_2O_2 (2.5 mmol/l) and 2,2′-azino-di-(ethylbenzthiazoline) sulfonic acid (2 mmol/l). After 30 min, the optical densities (OD) at 492 nm were determined using an ELISA reader.

2.3. Ultrasonic echocardiography

Echocardiography was performed with the rabbit under anesthesia using 3 mg/kg thiopental sodium (Tanabe Seiyaku Co.). The parasternal long-axis views were obtained using a 7.5 MHz transducer connected to a Hewlett-Packard Sonos 500 ultrasonic echocardiographic system (model 77010CF), with the rabbit placed in the lateral decubitus position.

2.4. Hemodynamic and histological analysis

At the end of each observation period, hemodynamic measurements were performed in the open-chest condition under anesthesia with chloral hydrate as described previously [4]. Hearts were then rapidly removed. Excised hearts were fixed in 10% formalin and embedded in paraffin, and both transverse and cross sections (3 μm thickness) were obtained. Sections were stained with hematoxylin and eosin and were subjected to light microscopic examinations. Planimetry was performed macroscopically on cross sections of the hearts to evaluate left ventricular (LV) muscle mass and cavity area and microscopically on 100 cross-sectioned myocytes to determine cross-sectional area per myocyte, using NIH Image. Immunostaining was also performed in order to detect IgG on cardiac membrane. Endogenous peroxidase was inactivated by treatment with methanol + 1% H_2O_2. After blocking with PBS supplemented with 3% BSA, each sections were incubated for 60 min with biotinylated goat anti-rabbit IgG. After three washes with PBS, the bound biotinylated antibodies were detected by the same method of ELISA.

2.5. Na–K-ATPase assay

The enzyme activity of myocardial Na–K-ATPase was determined by the colorimetric method. Membrane fractions were prepared as 50,000 g pellet as described previously [4]. Each membrane fragment was mixed with the reaction solution (100 mM NaCl, 10 mM KCl, 3 mM $MgCl_2$, 1 mM EGTA and 50 mM histidine, pH 7.2) at 4 °C. One hundred microliters of the membrane were mixed with 800 μl of the reaction solution and 100 μl of 30 mM ATP. For each sample, reactions with or without 2 mM ouabain were run in triplicate. We also determine the effects of purified IgG against myocardial Na–K-ATPase activity in each group. Myocardial membrane fragments were prepared from foreign healthy rabbits, and these Na–K-ATPase activities in the presence of 1 μg purified IgG were compared among the three groups. The IgG purification from rabbits serum was performed by protein A-agarose methods using the Affi-Gel Protein-A MAPS II Kit (Bio-Rad Laboratories, Hercules, California). The reactions were allowed to proceed for 2 h at 37 °C. Na–K-ATPase activity was expressed as inorganic phosphate produced 1 h/mg of membrane protein. The plasma and myocardial norepinephrine level was also determined by high-performance liquid chromatography.

2.6. Immunoblotting

Immunodetection of inhibitory G-protein (Gi) and Na–K-ATPase levels in the membrane fraction (20 μg) was performed using standard SDS-PAGE and immunoblotting techniques, as previously described [5]. Fixed samples were included on each gel as standard for quantification of the densities of each blot. Antisera against Gi (Santa Cruz Biotechnology) and Na–K-ATPase (Upstate Biotechnology, Inc.) were used as primary antibodies, and horseradish peroxidase-linked anti-rabbit IgG (Boehringer Mannheim) was used as a secondary antibody to detect individual protein

levels. The densities of each blot were quantified by densitometric scanning. Gi protein level was standardized by defining the mean density of membrane fraction from control rabbits as 1.0 densitometric unit. Na–K-ATPase levels were quantified by the relative intensity in comparison with 2 μg of porcine brain Na–K-ATPase. The specificities of antibody binding for each antigen were confirmed by neutralization assays using blocking antigens.

2.7. Statistics

Data are expressed as mean±S.E.M. Comparisons between three groups were performed by one-way ANOVA accompanied by a Bonferroni post hoc test when appropriate. Changes in OD on ELISA were analyzed using a repeated-measure ANOVA, whereas differences in mean values between the groups at a specific dose were determined by one-way ANOVA. Statistical significance was defined as $p<0.05$.

3. Results

OD values of ELISA in control group showed low throughout the observation period. In contrast, OD in beta and NKA group was high from the second through the sixth month, and there was no difference of OD between the two groups (Fig. 1).

Data on cardiac function are summarized in Table 1. Thickening of both the interventricular septum and the posterior wall was noted with a decrease in the LV end-diastolic dimension in beta and NKA group compared with control group on echocardiography (Fig. 2). Hemodynamic data demonstrated a relative bradycardia in only NKA group, and an elevation in LV end-diastolic pressure and a decrease in peak − d*P*/d*t* and cardiac output in both beta and NKA group. There was an increase in LV weight in beta and NKA group. Macroscopic examination of the hearts revealed LV hypertrophy, as evidenced by an increase in LV muscle mass and a decrease in the cavity area (Fig. 2). LV muscle mass corrected by the total cross-sectional area was increased in beta and NKA group. These macroscopic findings were endorsed by microscopic planimetry showing an increase in cross-sectional area per myocyte in both groups.

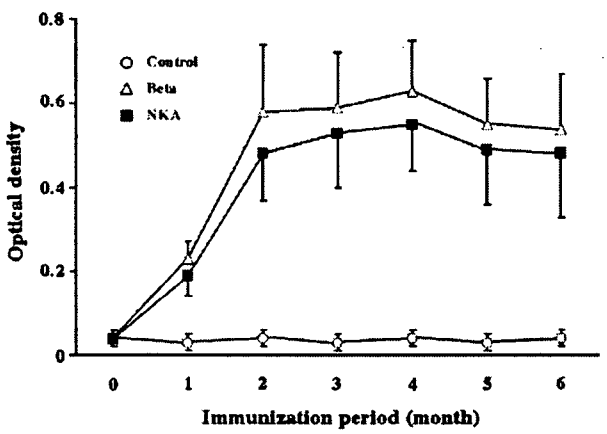

Fig. 1. ELISA of sera from three groups. Beta: a synthetic peptide corresponding to the second extracellular loop of beta1-adrenergic receptors, NKA: porcine cerebral cortex Na–K-ATPase, control: average of above both antigens. Data are expressed mean±S.D.

Table 1
Hemodynamic and morphometrical analyses

	Control	Beta	NKA
Ultrasonic echocardiography			
LV end-diastolic dimension (mm)	11.9±0.4	10.4±0.4*	10.5±0.4*
LV end-systolic dimension (mm)	7.2±0.4	6.9±0.3	7.0±0.3
Fractional shortening (%)	40±3	35±3	35±3
IVS wall thickness (mm)	2.6±0.1	3.3±0.2*	3.4±0.2*
LV posterior wall thickness (mm)	2.7±0.2	3.4±0.2*	3.4±±0.2*
Hemodynamics			
Heart rate (bpm)	253±9	254±8	213±7[a]
Aortic systolic pressure (mm Hg)	124±5	118±6	116±5
Aortic diastolic pressure (mm Hg)	90±6	92±5	91±4
LV end-diastolic pressure (mm Hg)	4.5±1.1	8.4±1.2*	9.4±1.1*
Peak + d*P*/d*t* (mm Hg/s)	4225±220	3975±175	4000±180
Peak − d*P*/d*t* (mm Hg/s)	3575±198	3060±159*	3025±162*
Cardiac output (ml/min/kg)	148±8	121±8*	120±7*
Weight			
Body weight (kg)	3.65±0.13	3.61±0.71	3.64±0.52
LV weight (g/kg)	1.42±0.02	1.54±0.04*	1.53±0.05*
RV weight (g/kg)	0.44±0.01	0.42±0.02	0.46±±0.02
Anatomic measurements			
LV wall area (mm^2)	117±7	138±7*	136±6*
LV cavity area (mm^2)	44±7	26±6*	25±7*
LV cross-sectional area (mm^2)	157±12	164±13	163±±11
LV wall area/cross-sectional area (%)	74±2	85±3*	84±2*
Myocyte cross-sectional area (mm^2)	250±15	338±25*	335±22*

IVS: interventricular septum, LV: left ventricle and RV: right ventricle.
[a] $p<0.03$ vs. control, beta.
* $p<0.03$ vs. control.

At 6 months, HE stain of organs except for heart had no significant pathological findings among the three groups. Histological findings of myocardium did not include any cellular infiltration in any group. However, myocardial hypertrophy with large nuclei, severe disorganization of the myofiber and interstitial fibrosis were present in the LV myocardium from beta and NKA group. Deposit of IgG around cardiac cell membrane was observed in beta and NKA group, although there was no stain in control group (Fig. 3).

Myocardial Na–K-ATPase activities were lower in the NKA group than other two groups, although plasma and myocardial norepinephrine concentrations had no difference

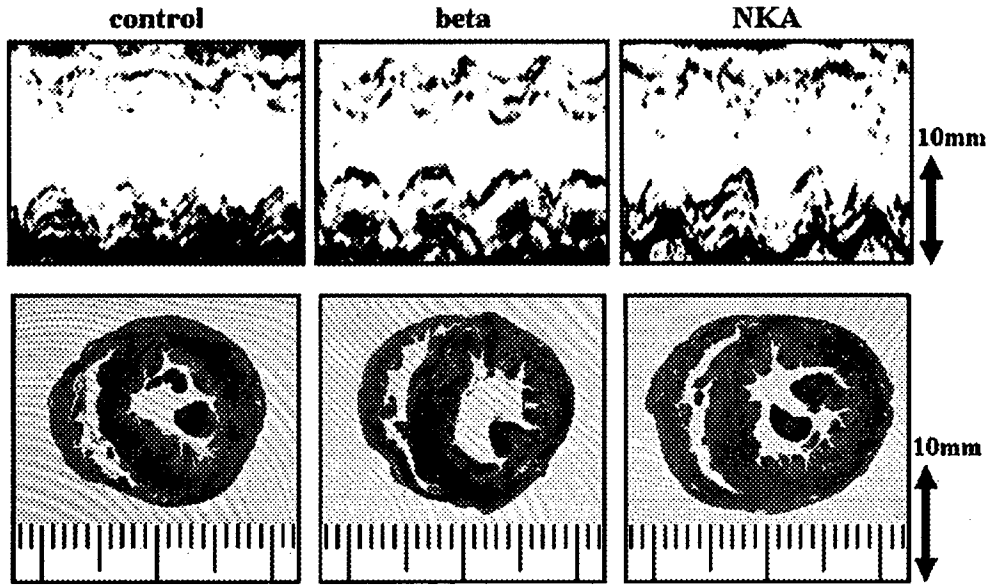

Fig. 2. Echocardiographic and macroscopic data from three groups. Beta, NKA and control; same as Fig. 1.

among the three groups. The effect of purified IgG against foreign healthy myocardium was compared among the three groups. Without adding IgG, Na–K-ATPase enzyme activity was 142 μM Pi/h/mg protein. The activity decreased by adding purified IgG from the NKA group, although there was no difference from control and beta group (Table 2).

Alpha3-isoform level of Na–K-ATPase was lower in the NKA group than control group, although there was no difference between beta and control groups. There was no difference in alpha1-isoform level of Na–K-ATPase in the three groups. Alpha2 level of Na–K-ATPase was also not different, either (data not shown). Gi protein level was higher in both beta and NKA groups than control group, without any difference between beta and NKA groups (Fig. 4).

4. Discussion

4.1. Cardiac hypertrophy induced by autoimmunity

Some previous observations have shown that repeated immunization using certain antigens corresponding to the second extracellular loop of beta1-adrenergic receptors and/

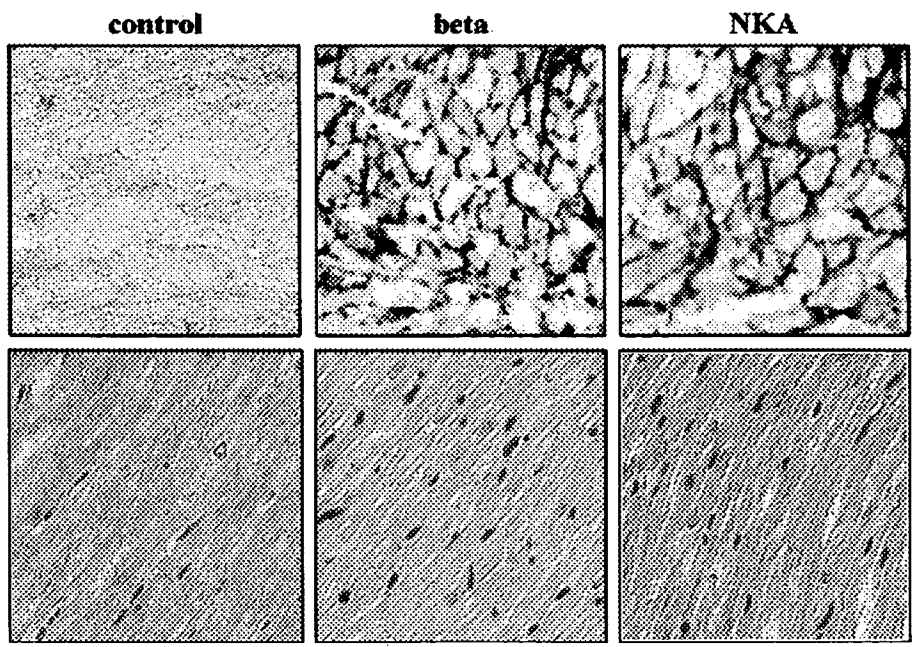

Fig. 3. Immunostaining of IgG and HE stain in myocardium from three groups. Beta, NKA and control; same as Fig. 1.